ISSN 2070-0504, Catalysis in Industry, 2022, Vol. 14, No. 1, pp. 66–85. © Pleiades Publishing, Ltd., 2022.
Russian Text © The Author(s), 2021, published in Kataliz v Promyshlennosti.

CATALYSIS IN CHEMICAL AND PETROCHEMICAL INDUSTRY

Modern Level of Catalysts and Technologies for the Conversion of Natural Gas into Syngas

L. G. Pinaeva[a], * and A. S. Noskov[a]

[a] *Boreskov Institute of Catalysis, Siberian Branch, Russian Academy of Sciences, Novosibirsk, 630090 Russia*

**e-mail: pinaeva@catalysis.ru*

Received June 4, 2021; revised June 30, 2021; accepted July 2, 2021

Abstract—The level of the main catalysts and industrial technologies for the conversion of natural gas into syngas further convrted into ammonia, methanol, and H_2 was analyzed. The main trends in their development, aimed at reducing the energy and resources consumption, were described including process flowsheets, catalysts, and sorbents at different stages of methane reforming and CO steam reforming.

Keywords: natural gas, methane reforming, catalysts, hydrogen, ammonia, methanol

DOI: 10.1134/S2070050422010081

INTRODUCTION

According to the annual BP Energy Outlook published by British Petroleum (BP) in 2020 [1], the share of natural gas (NG) in the total global energy consumption was 24% in 2019 and will remain almost unchanged for the next 30 years. This corresponds to its global consumption in 2018, equal to 3865 billion m^3/year, with prospects for growth to 5200 billion m^3/year by 2050, with gradually decreasing production growth rates from 1.7%/year (2014–2024) to 0.9%/year (2040–2050) [1, 2]. The list of countries with the largest NG production (billion m^3/year) in 2019 included the United States (951), Russian Federation (740), Iran (240), Canada (183), and China (175) [3].

The main component of NG is methane, whose content varies from 70 to 99% depending on the field [4]. It also contains ethane (3–8%), propane (1–2%), nitrogen (1–5%), CO_2 (1–2%); butanes, pentanes, helium, and hydrogen sulfide (<1% each); and occasionally even hexanes and heptanes. At present, NG is mainly used for fuel and energy purposes. Only a small proportion of it is used as a source of feedstocks for the production of basic chemical products: 1.5% in the United States and ~3% in Western Europe. Only China, whose energetics and chemical industry are mainly focused on coal conversion, uses up to 23% of consumed NG to obtain chemical products [4]. In Russia, the gas chemical sector receives no more than 5% of the total amount of consumed NG [6], primarily, for the production of NH_3 and CH_3OH, which are the basic chemical products that determine the development of the global petrochemical industry and will do this until at least 2050 [5]. At the first stage of all industrial processes for the production of NH_3, CH_3OH, and H_2, methane/NG is converted into a mixture of CO/CO_2 and H_2 (syngas, SG). This is the most expensive stage [7]. For example, in processes for the production of ammonia, its synthesis from N_2 and H_2 and separation take approximately one third of all capital investments in the project, and the remaining two thirds are invested in the production of H_2 [8]. In the majority of industrial processes for methanol production, the stage of the production of SG of the required composition amounts to 60–70% of its cost [9]. Therefore, the choice and optimization of process conditions for the production of SG are very important.

The present review considers the level of and trends in the development of commercial catalysts and technologies for the conversion of NG into SG used in the production of ammonia, methanol, and H_2.

1. MARKETS OF THE MAIN NG CONVERSION PRODUCTS

In 2018, the global demand for H_2 exceeded 73 million tons/year, and its largest consumers are oil refining (33% of the total demand) and production of ammonia (27%) and methanol (11%) [10]. It is expected that hydrogen production technologies will become even more important in the coming years in connection with plans for the transition of industrialized countries to environmentally friendly hydrogen energetics and to vehicles with fuel cells running on hydrogen.

Ammonia is the most important large-tonnage product (the overall production was ~173 million tons in 2017, of which 76–78% was provided by NG conversion [5, 8]) mainly used as a source of nitrogen for

the production of various fertilizers. By 2030, the production of ammonia is expected to reach ≈243 million tons/year (2.1%/year); the proportion of urea, mainly used as a fertilizer (83% of its applications), among the products of ammonia conversion will increase due to the possibility of minimizing CO_2 emissions formed at the reforming stage [8, 11, 12]. Russia has a capacity of over 19 million tons/year (40 units at 16 enterprises). Over the past six years, the production of ammonia increased by 22.7%; the total production being 17.7 million tons in 2018 [13, 14], the country is among the world leaders (more than 10% of world production) and second only to China, which will be the main country to provide growth in fertilizer production in the foreseeable future [8]. In accordance with the approved "Strategy for the development of chemical and petrochemical industry for the period of up to 2030," the potential of Russia for ammonia production will increase to 26 million tons. This will happen as a result of the construction of large production facilities at EuroChem North-West (2000 thousand tons/year), OTEKO (2500 thousand tons/year), National Chemical Group, and Nakhodka Fertilizer Plant (1800 thousand tons/year) using the technologies of the world's leading licensors [15–17]. All their products will be exported.

Currently, Haldor Topsoe, KBR, and ThyssenKrupp Uhde are the main developers of ammonia production technologies providing up to 70% of produced ammonia (excluding China) [8].

Methanol is one of the key petrochemical products, which accounts for ~19% of the market of these products [18]. Its production has more than doubled over the past 20 years, reaching 79–85 million tons in 2018 according to various estimates [5, 18–20]; and ~58% (2013) of the product was provided using NG as feedstock [19]. A slowdown in the growth rate of methanol production is not expected until 2050 [5]. In 2019, the production volume in Russia was ~4.7 million tons, which accounts for 5% of the global market of methanol, with more than 40% (~2 million tons) produced for export. Among the leaders with a total market share of ~84% are Metafrax, United Chemical Company Shchekinoazot, Sibmetakhim, and Tomet [21, 22]).

Data on the production capacities of different licensors are very different. According to the data of [23], Jonhson Matthey occupies a leading position with ~60% of the market. However, we believe that more reliable data were published in [24] about approximately equal total capacities of the operating plants licensed by Lurgi (27%) and Johnson Matthey (JM)/Davy (25%), with Haldor Topsøe approaching these (16% of the market).

In recent years, pure H_2 has become one of the important NG conversion products further used in various oil refining processes. A significant increase in the global demand of oil refineries for pure H_2, which reached 12.3 million tons/year in 2013 [25], was dictated by the growing requirements to the purity of automobile fuels. In 2013, the annual production of H_2 at 12 refineries in Russia amounted to ~500 thousand tons. This ensured the operation of 107 hydrotreating units and seven hydrocracking units. To meet the growing demand, 14 additional units were built with a total H_2 capacity of over 1 million tons by 2020, mainly for hydrocracking of vacuum gas oil [26, 27].

The Fischer–Tropsch process underlies many technologies for obtaining a mixture of a wide range of higher hydrocarbons (olefins, paraffins, cyclic and aromatic hydrocarbons), as well as oxygen-containing compounds (alcohols, aldehydes, carboxylic acids, ketones, etc.) from nonpetroleum feedstock. It is based on a catalytic reaction between CO and H_2, which proceeds in the temperature range 190–350°C at pressures from 20 to 45 kgf/cm^2. A large number of announced projects, including demonstration plants using Sasol, Shell, Axens, BP/Davy, ConocoPhillips, Rentech, and other technologies with a capacity from 3 to 1000 bpd [28]. However, currently only three large complexes are in operation: Oryx and Pearl in Qatar and Escravos in Nigeria, using Sasol and Shell technologies, with a total capacity of ~29 thousand tons per day (tpd). High volatility of oil prices in recent years led to the absence of further plans for construction of large facilities based on these technologies.

2. MAIN TRENDS IN THE DEVELOPMENT OF NG CONVERSION INTO SG

Three main technologies of NG conversion into SG have been implemented on an industrial scale, including multistage processes using steam and/or oxygen as an oxidizer: steam reforming, autothermal reforming, and partial oxidation, and various combinations thereof. Their main characteristics are given in Table 1. The choice and combination of processes in each case depend on several parameters (final product, production capacity, cost and availability of energy and feedstock resources).

2.1. Processes and Catalysts in Steam Reforming of Methane

2.1.1. Main characteristics of SG production by steam reforming of methane. The processes most frequently used in industry are based on steam reforming of methane proceeding by the reactions $CH_4 + H_2O = CO + 3H_2$, $\Delta H^\circ_{298} = 206$ kJ/mol; $CH_4 + 2H_2O = CO_2 + 4H_2$, $\Delta H^\circ_{298} = 165$ kJ/mol.

The use of these processes makes it possible to obtain SG with high H_2 contents. In the processes of the Uhde and Praxair companies, the H_2 concentration in the dried mixtures in SG (further used to obtain

Table 1. Key characteristics of for the developed technologies of NG conversion into SG [29]

Characteristic	Industrial technologies			Developed technologies	
	steam conversion	autothermal reforming (ATR)	non-catalytic partial oxidation (PO)	catalytic PO	CO reforming
T, °C	800–900	850–1300	1100–1500	900–1000	?
Pressure, kgf/cm^2	20–30	20–70	30–85	<5	?
Steam consumption	High	Low	Optional	Optional	Desirable
Demand for O_2	–	+	+	+	–
CH_4 reforming, %	65–95	95–99	95–99	96	?
H_2 : CO	3–6	1.6–2.5	1.6–1.7	1.8–2.0	≈1
Investment costs, %	100	65–68	80–110	–	–

ammonia and H_2) reaches 71–73% at 74–81% methane conversion, and the H_2 : CO ratio is 5.3–5.6 [29].

For the majority of the main licensors, modern processes for the production of SG using NG as a feedstock consist of the following main stages (Fig. 1):

(1) purification of natural gas from S and Cl compounds and olefins;

(2) steam reforming of methane;

(3) water gas shift reaction, WGS ($CO + H_2O = CO_2 + H_2$, $\Delta H^\circ_{298} = -41$ kJ/mol), after which the H_2 concentration increases to 73–76%, and the H_2 : CO ratio increases to 19–23;

(4) purification of the converted gas from carbon dioxide using chemical adsorption by aqueous solutions of various amines or by alkaline solutions based on hot K_2CO_3 (Benfield process of UOP, etc.), or using physical adsorption by methanol (Rectisol process of Linde/Lurgi companies), polyethylene glycol dimethyl ether (Selexol process of UOP), etc.;

(5) methanation of carbon monoxide and carbon dioxide residues on Ni/Al_2O_3 catalysts.

When H_2 is further used for the production of NH_3, the following stages are added to the technological scheme:

(6) compression of the nitrogen–hydrogen mixture;

(7) synthesis of ammonia at a pressure of 150–320 kgf/cm^2 and release of ammonia.

In some processes of ammonia production, as well as in the overwhelming majority (≈85% [30]) of modern enterprises producing H_2 for oil refining, a more economical pressure swing adsorption (PSA) technology is used, instead of stages 4 and 5, for removing CO_2 and CO, CH_4, and H_2O impurities from SG after WGS stage. In syntheses of SG subsequently used to obtain methanol, the WGS stage (3) and further stages are absent, and higher conversion value is achieved in the NG reforming reactor, at which H_2 : CO ≈ 3–3.5 is more suitable for the stoichiometry of the reaction of methanol formation [29].

The main licensors of these technologies are Linde (more than 200 plants with a capacity from 300 to more than 200 thousand m^3/h of SG); Air Liquide-Lurgi (45 reformers); Air Products (in alliance with Technip, more than 35 plants built over the past 20 years, with a total capacity of 57 million m^3/day of H_2); Kellogg Brown & Root (KBR, a division of Halliburton); Foster Wheller Corporation; Haldor Topsoe; Praxair; Technip (more than 200 plants); and TKIS Uhde (more than 60 reformers) [29, 31–34].

If the NG contains significant amounts of higher hydrocarbons, they can be converted into olefins in the heater before the reforming reactor, which quickly carbonize the catalyst. In modern processes, this problem is solved by introducing a preliminary reformer in the technological scheme, in which all higher hydrocarbons are converted in the temperature range 350–650°C [34–37]: $C_nH_m + nH_2O = nCO + (m/2 + n)H_2$.

This allows [34–36]:

— the amount of steam supplied to the main reactor to be significantly decreased, which reduces the operating costs;

— minimizing the problem of "hot spots" arising during the conversion of higher hydrocarbons in the main reactor;

— various refinery gases, as well as naphtha, including heavy naphtha (T_b = 200°C), with up to 30% aromatics, to be involve in the refining process which increases the process flexibility in terms of feedstock composition.

The steam reforming technology has a significant drawback: it is technologically difficult to increase the converter capacity to values exceeding 110 thousand m^3/h (for NG), which is achieved by increasing the number of tubes with a catalyst to 200–250. This is primarily

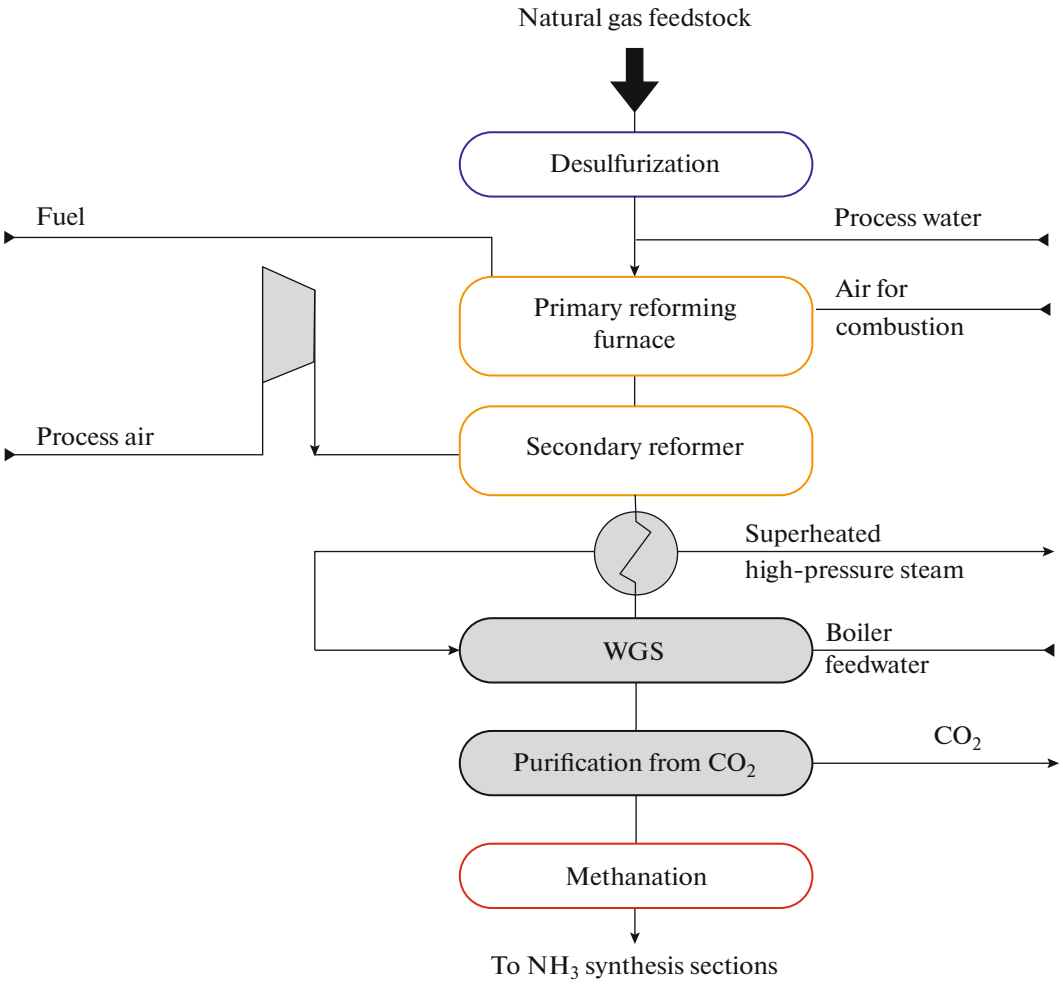

Fig. 1. Flow diagram of a unit for the production of SG in the ammonia production process (Uhde) using NG feedstock [13].

associated with the necessity of maintaining a high steam to NG ratio at the reactor inlet (2–3) to minimize the catalyst coking and also with the design of the furnace burners, which provides a spatially uniform temperature field on the reactor tubes [38]. An increase in the capacity of a single reformer to 200 thousand m^3/h for H_2 without any significant increase in its size became possible due to an increase in the process temperature to 1050°C in the High Flux Reformer at Haldor Topsoe as a result of the development of new materials for the tubes and more thermostable catalysts, as well as optimization of temperature gradients on the tubes [34]. Technip has reformers with close maximum performance. At a methanol plant in Qatar, Uhde has implemented the project of a reformer with 960 tubes.

Release of significant amounts of CO_2, which is practically not processed except in urea production, is another drawback, which will potentially restrict the use of the relatively simple and most efficient natural gas/methane reforming process in future.

2.1.2. Catalysts and adsorbents in SG production process. The majority of the stages of technological chains for the production of SG from NG (Fig. 1) require the use of catalysts or sorbents. Almost all manufacturers (Haldor Topsoe, Johnson Matthey, and Clariant) offer a full line of catalysts/sorbents with similar compositions.

(1) Natural gas purification stage. Natural gas generally contains impurities of various S (mercaptans, thiophenes, sulfides, H_2S, etc., up to 5.5 mg/m^3) or Cl (up to 1 ppm) compounds, as well as olefins, which lead to a dramatic decrease in the activity of any reforming catalyst. Thus, the limiting sulfur content in the gas after purification should not exceed 0.1, 0.05, and 0.01 ppm for catalysts of steam reforming, low-temperature WGS, and NG pre-reforming, respectively. Therefore, natural gas is purified from impurities in two stages [29, 39]. All S- or Cl-containing compounds, as well as olefins, are initially reduced to H_2S, HCl, and paraffins on $Co(Ni)–Mo/Al_2O_3$ catalysts at 370–500°C; the $Ni–Mo/Al_2O_3$ systems suit-

able for higher gas purification are used for processes with a pre-reforming stage. The main requirement to the support is the greatest possible specific surface area (up to 290 m^2/g for the Ni–Mo/Al_2O_3 catalyst KATALCO JM-61-6T). The next layers of adsorbent based on extrapure ZnO or a mixture of partially reduced zinc, aluminum, and copper oxides (Cu : Zn : Al = 1 : (0.6–3) : (0.3–1) [40]) prepared by co-precipitation remove H_2S from the flow, forming ZnS. To absorb carbonyl sulfide, an additional catalyst is installed, which generally consists of 90% ZnO, the remaining 10% being specially modified Al_2O_3 on which hydrolysis of COS occurs in water vapor present in the natural gas. Hydrogen chloride obtained after the hydrogenation stage chlorinates ZnO to $ZnCl_2$, which readily sublimes at $T > 260$°C. To prevent its deposition on the downstream steam reforming catalyst, leading to poisoning, and on heat exchangers (deteriorated heat removal, pipe rupture, reduced lifetime), a quard-bed based on γ-Al_2O_3 with supported potassium carbonate (Haldor Topsoe) or sodium carbonate is installed between the hydrogenation catalyst and ZnO for adsorption of HCl.

(2) Catalysts of pre-reforming and NG steam reforming stages. The reforming reactions are catalyzed by metals: Ni, Co, Pt, Pd, Ir, Ru, and Rh. Attempts to use nonmetal catalysts were unsuccessful because of their low activity [36]. Cobalt and noble metals (Pt, Pd, Rh, Ru) are more active than Ni in this reaction, and noble metals show greater resistance to coking [41–43]. The choice of nickel for industrial processes was dictated by the combination of low cost, high activity, and stability.

The stability of operation of these catalysts is generally attributed to their resistance to carbon deposition and the sintering of the active component [44]. In recent years, the catalyst coking problem was solved by replacing the Al_2O_3 support by mixed oxides Mg(Ca)–Al–O with higher basicity. The catalyst strength is enhanced due to the absence of pure MgO (CaO) or calcium-enriched $12CaO–7Al_2O_3$ and $3CaO–Al_2O_3$ phases, which are easily hydrated, especially during the reactor start and shutdown, and are poorly recovered under the process conditions [45]; the duration of the start-up procedures also decreases due to the absence of these phases [39, 45, 46]. To prevent the formation of inactive Ni–Al–O spinel during the preparation of Ca–Al–O supports, Sud Chemie (currently part of Clariant and Haldor Topsoe) pay special attention to complete removal of Al_2O_3, which is judged by the formation of the gibonite $CaAl_{12}O_{19}$ phase [47, 48]. An increase in the specific surface area of the support during the formation of $MgAl_2O_4$ or various Ca aluminates leads to stabilization of fine Ni particles [49]. Further increase in Ni dispersion is possible if the support is impregnated with La, Ce, Ti, or Zr salts before the deposition of the active component. Thus, after 250 h run, the activity of the catalysts modified with Ti and La (~6 wt %) was 20 and 100%, respectively, higher than that of the Ni–Ca–Al–O catalysts prepared by the standard method [45]. The addition of TiO_2 to the RC-67 TITAN™ catalysts (Haldor Topsoe) provide higher resistance of these catalysts to sintering compared with that of basic catalysts based on calcium aluminates [48].

Resistance to coke formation is additionally increased by introducing an alkaline promoter, generally KOH, which additionally catalyzes the reactions between the deposited carbon and H_2O vapors. However, the high volatility of KOH under the reaction conditions requires special methods for fixing potassium in the catalyst. In one of the latest Haldor Topsoe patent applications, potassium is introduced directly in the molding paste at the stage of support preparation, as a result of which it enters the Mg–Al–O lattice, forming the crystalline phases $K_{1.62}Mg_{0.62}Al_{10.38}O_{17}$ and $K_2Mg_4Al_{30}O_{50}$. Due to this, the support plays the role of a reservoir that maintains the concentration of the alkaline additive on the surface at a constant level (Fig. 2a) and ensures greater stability of these samples compared with that of the samples obtained by conventional methods (Fig. 2b) [50, 51]. However, the introduction of alkaline and alkaline earth additives lowers the catalyst activity [29, 52]. Therefore, in modern processes, layer arrangement of catalysts is used [47, 53, 54], which ensures their maximum activity throughout the run:

— with more coking-resistant catalysts based on Mg(Ca)–Al–O installed in the frontal layers and more active catalysts based on unmodified α-Al_2O_3 installed after them;

— with decreasing content of the alkaline additive in the catalyst along the bed length [47, 54].

For catalysts based on $MgO–Al_2O_3$, for which the reduction of NiO to the metallic state under the reaction conditions occurs especially slowly [45], Haldor Topsoe proposed catalysts with pre-reduced Ni. They are characterized by markedly higher activity than that achieved by reducing the catalyst in the reactor. These catalysts are installed before the corresponding unreduced catalyst, and hydrogen that formed on them activates downstream catalyst, which significantly reduces the start-up time of the apparatus [54].

In recent years, there were almost no patents on the improvement of methods for the preparation of catalysts for large-scale reactors. Nevertheless, publication activity dealing with the search for effective reforming catalysts, especially those working in mixtures with a reduced H_2O/CH_4 ratio, in scientific journals has not declined. These publications were briefly analyzed in the review [55].

The different conditions in the reactors of preliminary and main reforming determine the optimum physicochemical characteristics of the catalysts used in them (Table 2).

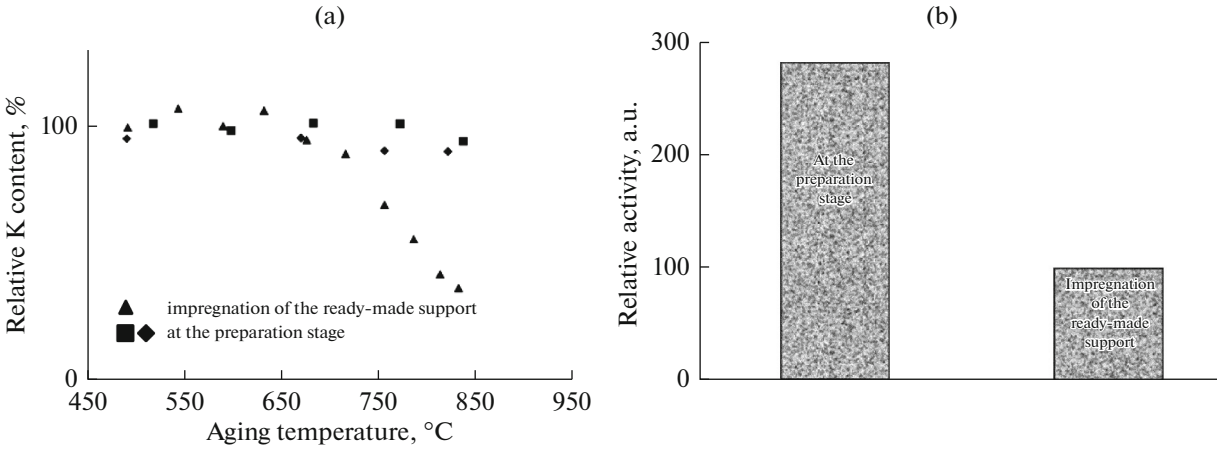

Fig. 2. Effect of the method by which K is introduced in the samples on the (a) K content after various treatments and (b) activity of the samples after a long run in an NG steam reformer.

To ensure the required activity at lower temperatures, the pre-reforming catalysts generally contain much more nickel (up to 45 wt %) than those of the main reforming (≈12 wt %) [29, 34, 57]. In the first-generation pre-reforming catalyst RKNGR (Haldor Topsoe) with 25 wt % nickel, the required activity determined by the particle size and, accordingly, the specific surface area of nickel (up to 15 m^2/g of catalyst) was achieved by lowering the calcination temperature of the carbonization-resistant support based on Al_2O_3 modified with K_2O [34]. The high sintering resistance of Clariant catalysts with a markedly higher Ni content (≈44%) is due to the fact that during codeposition in the presence of K (≥0.05% in the final catalyst) Ni and Al form a well-crystallized structure with crystallization water inclusions. At present, the majority of companies use aluminum–magnesium spinel as a support with a La addition that stabilizes its structure, or calcium aluminate modified with Cr_2O_3, and SiO_2 to improve the strength characteristics [29]. Air Products patented catalysts with significantly lower (up to 20 wt %) nickel supported on calcium aluminate [37, 58]. The lower activity of these catalysts compared with commercial ones can be compensated by their

Table 2. Comparison of operating conditions and designs of preliminary and main reforming catalysts [29, 56]

Characteristic	Main reforming	Pre-reforming
Temperature, °C	500–850	400–550
Space velocity of NG feeding, h^{-1}	3000–8000	3000–8000
H_2O : methane, mol/mol	2.5–3.2	1–3.2
Pressure, kgf/cm^2	20–40	20–40
Heat transfer requirements	The catalyst shape should provide flow turbulization and radial heat transfer. Complex forms	The reactor works in an adiabatic mode. Simple geometry, providing low pressure drop in the bed
Catalyst activation	Generally supplied in the oxidized state	Generally supplied in the reduced and afterward passivated form required for easy activation and high resulting Ni surface
Ni surface	≈2 m^2/g	Up to 15 m^2/g
Thermal stability of the catalyst	Very high	High
Promotion	Often promoted to prevent carbonization	Promoted sometimes to avoid coking
Pressure difference in the bed	Shape optimization to provide high heat transfer and geometrical surface	The maximum geometrical surface area is required

use at higher temperatures. Their higher sintering resistance is facilitated by the formation of a bimodal porous structure with a large number of transport pores. A decrease in sulfur adsorption on such catalysts at higher temperatures also prolongs their lifetime. However, currently there are no catalysts with lower nickel contents on the market. It is also known that the particle size of the active component is stabilized in the presence of vanadium additives [59].

To facilitate the activation of catalysts in the pre-reformer, they are often supplied in a pre-reduced and then passivated state. As a result of the partial reoxidation of a catalyst preliminarily reduced at $T > 550$°C, a thin film of inert NiO forms on the catalyst surface, which is easily reduced under the conditions of a pre-reformer, but allows such catalysts to be safely stored in air [37, 56]. The absence of problems with mass transfer in the pre-reformer allows the use of catalysts with a simple geometrical shape (granules, multichannel cylinders) with a size sufficient to ensure low pressure drop across the bed. In the main reactor, however, a complex geometrical shape of the catalyst is required, which ensures flow turbulization and an increase in the heat transfer over the bed [60]. Thus, in 2017, Clariant started to produce the ReforMax 330 LDP Plus and ReforMax 210 LDP Plus catalysts in the form of eight- and ten-channel flower-shaped blocks, providing a higher total surface area and a lower (≈20% compared to multichannel cylinders of the same size) pressure drop across the bed, which makes it possible to increase the load on the reactor by ≈11% [61, 62].

(3) Catalysts of the WGS stage. In WGS reaction used to obtain additional amounts of hydrogen, the equilibrium conversion of CO increases at lower temperatures. However, sometimes the catalyst activity in the low-temperature region is not high enough to reach equilibrium. In addition, the reaction performed at high temperatures allows the use of generated heat to create sufficient water vapor pressure. Therefore, in industry, this process was historically implemented in two temperature intervals. Sometimes the schemes combine both temperature ranges. In this case, in a high-temperature reformer operating in the ranges of temperatures 320–450°C and pressures 25–35 kgf/cm^2 on catalysts consisting mainly of Fe_2O_3 stabilized by CrO_3 (8–14 wt %) [63], the residual CO content in the mixture is 3–4%. Occasionally it is possible to reduce the CO concentration in the products to 1–3%, which depends on the number of catalyst beds used [64, 65]. In the subsequent low-temperature reforming reactor operating in the temperature range 210–240°C, the CO content further decreases to 0.1–0.3% in the presence of $CuO–ZnO/Al_2O_3$ catalysts.

The addition of chromium to Fe_2O_3 stabilizes Fe_3O_4 (magnetite), formed under the reaction conditions as a result of the reduction of hematite, morphologically and structurally in the spinel structure with a composition $Fe(Fe_{2-x}Cr_x)O_4$ characterized by a specific surface area of 10–50 m^2/g [66]. The main disadvantage of these catalysts is very labor-consuming and wasteful production using the deposition method. The highly viscous and gelatinous precursors formed during deposition—iron hydroxide and iron oxyhydrate—are difficult to filter and wash clean. The presence of sulfur in the final catalyst lowers its activity when the source of iron is iron sulfate, its most accessible and cheapest reagent. Under conditions with a low vapor to CO ratio, excessive reduction of iron oxide to metal, which is a catalyst of the Fischer–Tropsch synthesis, is possible, forming methanol and hydrocarbons. Its strength characteristics also decrease. Therefore, under high-temperature conditions, it is always necessary to have an excess of H_2O, which additionally increases the operating costs of the process. In addition, under the reaction conditions, the catalyst contains up to 2 wt % chromium in a hexavalent state [67], which is highly toxic and has carcinogenic properties. Therefore, in the 2000s researchers started to search for alternative additives capable of stabilizing the α-Fe_3O_4 phase. The catalysts promoted with calcium, strontium, barium, zinc, thorium, manganese, magnesium, and gallium oxides had low activity. Optimization of the preparation procedure, as well as the introduction of copper and cobalt additives, slightly increased the activity [68]. The initially active promoted PbO and iron oxide catalysts supported on CeO_2 and Al_2O_3 quickly deactivated during the reaction and were very sensitive to the presence of even trace amounts of sulfur in the feedstock [67]. Haldor Topsoe patented the compositions based on mixtures of magnesium, manganese, aluminum, and zirconium oxides and lanthanides as catalysts on which methanation does not occur [69], and promotion of manganese–zirconium oxides with copper or silver led to an increase in activity [70]. In the latest modifications of catalysts (e.g., ShiftMax 120 HTC catalysts from Clariant [71]), additives of copper are often used (up to 10%), which stabilizes in the metallic state under the process conditions and maintains iron in the optimum oxidation state [66].

All licensors of low-temperature WGS technologies offer catalysts based on copper–zinc spinels supported on Al_2O_3. In addition to their high sensitivity to the sulfur content in the feedstock, they quickly lose strength in the presence of liquid water [52]. In this temperature range, the methanation rate is insignificant; however, the reaction of methanol formation can proceed. To minimize this reaction, alkali metal (Na, K, Cs) additives are used, of which cesium is the most effective additive used in Haldor Topsoe's LK-823 or LK-853 FENCE™ catalysts. It is generally known that WGS reaction on these catalysts is structurally insensitive: the active component is copper in the metallic state or Cu(1), and the reaction rate depends on its total surface area regardless of the Al : Zn ratio, crys-

tallite size, and the total copper content in the catalyst. The role of ZnO in such systems is still under discussion. Some researchers believe that ZnO plays an active role, stabilizing active Cu^{1+} particles in the ZnO matrix, or the activity increases due to the synergistic effect with copper metal particles. Others believe that ZnO simply as a structural additive helps to maintain copper in a finely dispersed state [72]. In addition, the presence of zinc oxide in a free form in the catalysts makes them resistant to sulfur poisoning due to the high chemisorption capacity of any organosulfur compounds and H_2S [53].

To ensure the maximum dispersion of the active component, the catalyst is prepared by coprecipitation from aqueous solutions of metal salts (nitrates, sulfates, or acetates) under strict control of pH, temperature, rate of addition of reagents, etc. The main precursor of the active component is hydrotalcite [73–76], including with coordinated water (Cu, $Zn)_6Al_2(OH)_{16}CO_3{\cdot}4H_2O$ [77]. Methods for the preparation of the catalyst which make it possible to strictly control its content in the sample have been patented [74–76, 78]. An effective method to increase the strength and activity of catalysts usually loaded into the reactor in a pre-reduced form is elimination of the stage of their calcination in air after drying [79]. In 2016, Johnson Matthey patented a specific procedure for the drying stage, which consists in maximally complete removal of water without decomposition of copper compounds to oxides [80]. One way to increase the dispersion of copper and zinc patented by BASF includes coprecipitation of Cu and Zn on finely dispersed alumina [75, 81].

The review [82] describes the attempts to replace Zn and Al with other structural additives, which stabilize copper in a finely dispersed state, primarily, in the form of spinels. Among various copper-based spinels, $CuMn_2O_4$ and $CuAl_2O_4$ were characterized by a noticeably higher specific rate of CO conversion than the commercial $Cu/ZnO/Al_2O_3$ catalyst [83]. Nevertheless, there are no data on the industrial application of Mn-containing catalysts, which may be explained by their low stability. Thus, the activity of copper-containing catalysts can be increased only by increasing the temperature. However, this requires an increase in their resistance to sintering under hydrothermal conditions. Recently, L'Air Liquide patented the procedure for the calcination and subsequent reduction of hydrotalcite Zn–Cu–Al–O, which ensures the equilibrium value of CO conversion on the catalyst at 250–350°C already at a contact time of 1 s and the absence of methanol and other undesirable oxygenates in the products [84, 85]. The ShiftMax 300/500 catalyst for medium-temperature conversion offered by Clariant is possibly prepared based on this patent.

Work on the use of systems based on CeO_2 or TiO_2, characterized by high redox capacity and surface area under reaction conditions, as catalyst supports for both high- and low-temperature ranges has been under way over the past 20 years [86–91]. Initially as active as the commercial samples [86, 89, 90], the Pt(Pd, Re)/CeO_2 systems become quickly deactivated, which was attributed by various authors to the irreversible reduction with hydrogen or decreased metal surface area. Therefore, they cannot be regarded as promising for industrial applications until the stability problems are solved.

In 2012 Haldor Topsoe patented the Zn–Al–O catalyst (Zn : Al = 0.65–0.7), which is a mixture of $ZnAl_2O_4$ and ZnO under reaction conditions. Promotion with an alkali metal (K, Cs) provides a decrease in the methanation rate at low steam : CO ratios in the initial mixture, and the activity of this catalyst under certain conditions is even higher than that of the commercial Fe–Cr–O catalyst. It has increased thermal stability and does not require ultrafine purification from chlorine and sulfur [92]. This patent served as the basis for the currently produced LK-813 and LK-817 catalysts operating in the medium temperature range from 190 to 330°C, as well as for SK-501 Flex™ aimed to replace the Fe–Cr–O catalyst in units operating at low steam/carbon ratios (<2.6) [93]. Thus, the manufacturer guarantees stable operation of SK-501 Flex™ catalysts in the SynCOR Ammonia™ process (steam : CO = 0.6) for at least 28 months [94]. The use of LK-813(817) catalysts makes it possible to direct the gas after the steam reforming stage directly to the PSA unit.

As in many industrial processes, layered charge of catalysts started to be widely used in WGS reactors, which ensures the optimum occurrence of individual reactions, including the composition of feedstock and process conditions. In the case of three-layer charge of LK-813(817) catalysts, LK-817, characterized by good water resistance and high chlorine capacity, is installed in the upper layer; LK-813, which is more active than LK-817, is installed inthe middle layer; and LK-817, which is more heat-resistant, in the lower (high-temperature) part of the reactor.

(4) Catalysts of the CO methanation stage.

For the methanation stage at which residual CO (≈0.5%) is removed, the majority of manufacturers (Haldor Topsoe, Johnson Matthey, Clariant) offer catalysts with a composition of ≈30% Ni/Al_2O_3, which are often preliminarily reduced in order to decrease the duration of start-up regimes. According to the data of Johnson Matthey, their lifetime reaches 20 years [95]. This is probably why the KATALCO JM 11-4 and KATALCO JM11-4R (in reduced form) catalysts proposed by them for this stage had not changed since 2007 until at least 2021 [96]. At the same time, the lack of new developments may be explained by the decreased number of facilities/plants for their use because of the development of more active catalysts for CO steam reforming and the wider use of PSA technologies.

(5) Sorbents for the PSA stage.

UOP, Air Liquide, and Linde are the main licensors of PSA technologies, which allow isolation of up to 95% hydrogen (with more than 99% purity) from the gas mixture [34, 97, 98]. This degree of purification is achieved by layer-by-layer (to three or four layers) filling of reactors (up to 16 in parallel in modern schemes) with packages of sorbents of different functionalities, whose lifetime reaches 10 years. Table 3 shows the typical sorbents used to remove carbon oxides, nitrogen, water, and other impurities in SG.

The search for more effective sorbents does not stop. The work is aimed at expanding the temperature ranges of operation [100, 101] and improving the sorption capacity, especially in the presence of H_2O, by modifying the surface or optimizing the porous structure. Thus, the sorption capacity, as well as the selectivity of activated carbon (most widely used due to its structural stability and low cost) with respect to CO_2 [102, 103], additionally increase after its treatment with mixtures of monoethanol- and methyldiethanolamine [104] due to the chemical interaction of the basic sites of the surface with CO_2, which has acidic properties. The total surface area is increased and the microporous structure develops due to treatments in the CO_2 flow at elevated (up to 900°C) temperatures [105].

In recent years, the attention of researchers has been attracted by high-surface-area metal-organic framework structures (MOFs) and zeolite-like imidazolate frameworks (ZIFs), some types of which (MOF-74, MOF-177, UTSA-16, MIL-53, MIL-125, HKUST-1, ZIF-8, ZIF-90, ZIF-95, and ZIF-100) demonstrated high efficiency of separation of undesirable impurities from gases released after the WGS stage [106–111]. Their sorption capacity with respect to CO_2 at high pressures is additionally increased due to immobilization of various functional groups, primarily, organic amines and hydroxyls, on the pore surface, or to formation of coordination unsaturated metal sites [112]. Some of them, for example, the relatively inexpensive MOF UTSA-16 ($[K(H_2O)_2Co_3(cit)(Hcit)]$, H4cit = citric acid), which can be pelletized into relatively stable pellets without losing its sorption characteristics, are comparable to zeolites in their performance [113–115]. Al-Naddaf et al. [116] developed a simple method for the synthesis of a composite 5% zeolite-5A–95% MOF-74, a zeolite base with coordinated MOF fragments, which is promising from the viewpoint of application in industrial units for PSA. It is characterized by a significantly higher sorption capacity for CO_2, CO, CH_4, and N_2 compared with that of individual compounds and by high adsorption selectivity with respect to H_2. The authors explained this by an increase in the surface area and pore volume of the composite (by 27 and 29%, respectively, relatively to the starting MOF) as a result of the formation of mesopores at the zeolite–MOF interface.

Table 3. Typical sorbents used for removing various mixture components during purification by the PSA technique [99]

Adsorbate	Adsorbent
CO_2	Activated coal, Narrow-pore (5Å) zeolites, lithium zirconate, CaO
CO	Cu(I)
H_2O, hydrocarbons	Highly porous silica gels or aluminas with high surface areas
C_3–C_4	
CO_2, N_2, CH_4	Titanium silicates

2.2. Processes and Catalysts for SG Production by Autothermal Reforming of Methane

The use of heat released at the methane oxidation stage ($CH_4 + 2O_2 = CO_2 + 2H_2O$, $\Delta H^\circ_{298} = -801$ KJ/mol) for one-pot endothermic steam reforming reaction made the autothermal reforming (ATR) process very energy-efficient. Both reactions proceed at 1100–1300°C (frontal catalyst bed). Under these conditions, efficient mixing of feedstock before feeding to the burner with temperatures of ~2500°C is critical for the catalyst lifetime and the material of the reactor itself. Unlike the tubular steam reforming reactor, the ATR can be easily scaled up to the highest capacities. Progress in increasing the energy efficiency of the process is mainly associated with work on the design of efficient gas mixers, as well as the development of schemes that allow work with mixtures with high oxygen contents (e.g., TKIS's Uhde processes). The special design of recently developed burners (the main licensors are Lurgi, Haldor Topsoe, Kellogg Brown & Root) made it possible to minimize the formation of nitrogen and carbon oxides and to reduce the vapor : C and O_2 : C ratios at the reactor inlet. At the optimum content of O_2, feedstock, and steam in the mixture and under ideal reaction conditions, the theoretical efficiency of the process is higher than that of steam reforming, 95% vs. 90% [29]. However, because of the markedly higher temperature, especially in the frontal layers of the reactor, there may be problems with the catalyst sintering and loss of the active component and support as a result of the formation of highly volatile nickel and aluminum hydroxides. The problem of deactivation and increased layer resistance is solved by installing catalysts with supports with additives or those based on zirconium oxide in the frontal layers [117, 118], and by replacing some part of Ni with a platinum group metal, e.g., rhodium [118]. One of these methods was evidently used in the KATALCO 89-6Q catalyst (Johnson Matthey), designed for operation in the frontal layers of ATR reactors [119]. It is

also known that the active component of the similar RKA-10 catalyst from Haldor Topsoe is an alloy of Ni and a platinum group metal [120].

Because of the insufficiently high H_2 concentration and H_2 : CO ratio (Table 1) in SG for NH_3/H_2, ATR reactors are most often used for secondary reforming of partially converted SG in order to increase the process capacity. The choice and combination of reactors for various types of reforming for the production of SG are determined by the final product and production capacity.

2.3. SG Production by Partial Oxidation of Methane

The production of SG using the partial oxidation reaction in the absence of catalysts has the following limitations [29]:

— The high reaction temperature (1100–1500°C) and pressure (up to 75 kgf/cm^2) (Table 1), necessary for the reaction to proceed mainly to CO and H_2, increase the requirements to the structural materials of the reactor and make the process more energy-consuming.

— Due to the more efficient full oxidation of H_2 compared with that of CO, the H_2 : CO ratio generally lies in the range 1.7–1.8. Accordingly, to obtain SG for NH_3/H_2, it is necessary to increase the contribution of the WGS stage, which leads to a significantly higher cost of the process.

— The need to use pure oxygen as an oxidant reduces the economic characteristics of the process.

— The mixtures of CH_4 and O_2 are explosive in a wide range of conditions.

The use of supported catalysts based on Ni, Rh, Pt, and Ru, on which the H_2 and CO selectivities are up to 96–99% at H_2 : CO = 1.8–2.0 and 96% conversion of methane, makes it possible to lower the temperature process to 800–1000°C (Ni) (Table 1) and even 500–600°C (Ru). As all the results were obtained at millisecond contact times, when developing large-scale reactors it will be necessary to solve the problem of heat removal in the reactor, which will minimize gas-phase and secondary reactions. Deactivation of the catalyst as a result of quick carbonization and sintering are the main risks that determine its service life under high-temperature conditions with a substoichiometric oxygen content, especially in the absence of H_2O or at its low content in the reaction mixture.

2.4. Developed Processes of Carbon Dioxide Reforming of Methane

The official presentation of a plan for the formation of a carbon-neutral space in EU countries in 2019 (European Green Deal), which provides for a reduction in greenhouse gas emissions by at least 50% by 2030 compared to the level of 1990, requires a fundamental change in the existing technological order. This includes all-round rejection of technologies that lead to CO_2 release.

Therefore, as applied to SG syntheses for various purposes, studies on the possibility of methane reforming using CO_2 are attracting more interest: $CH_4 + CO_2 = 2CO + 2H_2$, $\Delta H^\circ_{298} = 247$ KJ/mol.

The composition of SG (H_2 : CO ≈ 1) obtained in accordance with the reaction stoichiometry is very suitable for its further use in the Fischer–Tropsch synthesis of liquid hydrocarbons, including aromatics, and valuable oxygen-containing compounds.

However, their industrial implementation is questionable because of the:

— obviously more stringent conditions in view of the higher stability of the CO_2 molecule compared with that of H_2O;

— quick carbonization, especially in the absence of H_2O, of the most economical nickel catalysts because of the side reactions of CH_4 decomposition and CO disproportionation, as well as their sintering, under almost all conditions;

— the need to use expensive catalysts based on platinum group metals (Ru, Rh, Pt, Pd) characterized by high resistance to carbonization apart from high activity [121].

In recent years, the active search for catalysts not containing platinum group metals showed that bimetallic catalysts based on Co–Ni, Mo–Ni, Fe–Ni, Cu–Ni, In–Ni, Sn–Ni, Co–Mo, and Cu–Mo alloys are most promising. The effective removal of carbon from the surface in such systems can be explained by the higher oxygen affinity of the modifying element (Co, Co–Cu, In) than that of Ni or Mo, which allows oxygen to be incorporated into Ni(Mo)–C structures, or by the cyclic processes of formation and destruction of alloys (Ni–Fe) under reaction conditions. The electron transfer from less electronegative Co or In to Ni stabilizes the bimetallic nanoparticles under reduction conditions and, in the case of $In–Ni/SiO_2$ catalysts, additionally leads to a weakening of the ability of Ni to activate the C–H bond followed by deep cracking of methane [122, 123].

Another important factor that provides high dispersion of Ni is the possibility of particle distribution in the mesopores of supports with a high specific surface area (SiO_2, MCM-41, SBA-15) due to the spatial distribution or metal interaction with the support, which prevent sintering [124–127]. In this case, it is especially preferable to use the ability of nickel to enter the spinel or perovskite structure [128–132] and leave the lattice in a reducing atmosphere under reaction conditions, thus forming nanoparticles stabilized by the interaction with the surface [128, 131, 133–136]. Mesoporous supports based on silicates and Al_2O_3,

however, suffer from increased coke deposition because of the acidic nature of the surface and often require additional promotion with noble metals [137, 138]. As in the case of steam reforming of methane, the problem is solved by using basic supports, such as Mg–Al spinel [139–141]. Resistance to coke formation and activity additionally increase for highly defective spinels with a developed mesoporous structure and large pore volume due to the fact that nickel leaves the lattice in a reducing atmosphere and forms nanoparticles, as it does in perovskites [142].

Recently, particular attention has been paid to supports based on ZrO_2 [143–146], whose structural characteristics (high thermal stability and strength, stable phase composition) are well suited for the conditions of reforming reactions [144, 147–149]. The resistance of these catalysts with fine nickel particles to filamentary coke formation [150, 151] and high stability under reaction conditions [151] are explained by the formation of extended Ni–O–Zr interphase boundaries, which promote carbon removal. A similar effect is produced if the size of ZrO_2 particles decreases [149]. ZrO_2 used as a promoter additionally increases the basicity of Ni–Mg–Al–O catalysts prepared from hydrotalcites [146, 152]. This leads to increased adsorption of CO_2 and, accordingly, to the removal of carbon from the surface [153]. Nevertheless, under reaction conditions, zirconium is gradually reduced to Zr^{1+}, as a result of which the surface content of Ni^0 and dispersion of nickel particles decrease. Modification of Ni–ZrO_x catalysts with manganese stabilizes zirconium in the oxidized state and prevents nickel from sintering [154]. A similar effect of Mn addition on the dispersion of nickel particles and decreased coke deposition in its presence, related to an increase in the concentration of mobile oxygen, including in surface layers, was observed for nickel catalysts with various supports [147, 155–159].

Cerium oxide CeO_2 is an alternative support, in which the high mobility of oxygen provides its spillover to the neighboring metal sites, where it participates in the gasification of carbon precursors [160]. Accordingly, the structure and length of boundaries between the metal particles and CeO_2 are the determining factors for the activation of reagents and the removal of carbon particles from the surface [161, 162]. The main strategy used to prevent inevitable coke deposition on the CeO_2 surface [163–165] during long runs in the absence of water vapor is the introduction of another cation in the crystal lattice of fluorite or its deposition on the surface of a more basic oxide (ZrO_2, Al_2O_3, La_2O_3, SiO_2) [166–168]. In the latter case, surface defects form at the interface, generating oxygen vacancies, on which the adsorption and activation of CO_2 is facilitated and followed by dissociation to CO and O* involved in the removal of carbon precursors [169]. Thus, the rate of carbon deposition on the Ni/CeO_2–Al_2O_3 and Ni/CeO_2–SiO_2 catalysts, in which the support was prepared by deposition of Ce on the Al_2O_3 (SiO_2) surface or by coprecipitation, was significantly lower than on the Ni/Al_2O_3 or Ni/SiO_2 samples. The activity of the modified CeO_2 samples remained almost unchanged or increased [169–172]. The influence of the preparation procedure on the activity and stability of catalysts based on CeO_2 was analyzed in detail in the review [173].

Thus, if interest in this process does not decline in the near future, it is logical to expect the appearance of industrial catalysts, at least for the variant with dosed steam supply to the reaction mixture.

2.5. Main Trends in the Development of H_2 Production Processes (Including for NH_3)

Since the introduction of the first processes, energy consumption in NH_3 syntheses has decreased by 45%: from 11 to 6.0 Gcal/t_{NH3} in the best processes [8, 13], which is largely due to the optimization of H_2 production technologies. The consumption of NG, including heating costs, in modern processes does not exceed 900 m^3 of NG/t_{NH3} (according to the stoichiometry of the reactions, 660 m^3 of NG is required at all stages at 100% yield) [13]. Several developments have been implemented on an industrial scale, due to which the material and energy consumption is reduced.

The use of a secondary air reformer (usually absent in H_2 production processes, as well as in the Linde Ammonia Concept (LAC™) process) in addition to the main steam reforming reactor at a constant unit capacity makes it possible to:

— obtain pure N_2, which is necessary for the subsequent NH_3 synthesis stage, by the reaction between atmospheric oxygen and H_2;

— remove as much as possible methane that remained after the reforming stage;

— reduce the volume and load on the primary reformer, which significantly lowers the amount of loaded catalyst, increases the lifetime of the catalyst and tubes (Table 4), and reduces the cost of routine maintenance of the unit.

The addition of a secondary reforming stage, in turn, allows an increase in process productivity without increasing the volume of the steam reformer.

The most important improvement of flow charts, which allowed a dramatic increase in process economics in recent years, concerns the use of additional heat exchange reformers by Topsoe, KBR, and other companies. A reactor of this type has a capacity of up to 40 thousand m^3/h; this is a heat exchanger, whose tubes are filled with a steam reforming catalyst, some part (up to 20–30%) of the initial mixture is fed through a bypass, and the heat required for the reaction is provided by passing SG after the steam or sec-

Table 4. Comparison of the characteristics of primary steam reformers in the standard ammonia synthesis and KBR's Purifier™ process with an added secondary reformer [8]

Primary reformer	Standard	Purifier™
Number of tubes	100%	65%
Outer diameter of tube, mm	110	125
Heat flux, kcal/(h m^2)	76000	55000
Gas temperature at the outlet, °C	800–840	700
Lifetime of tubes, years	10	12–25
Total amount of catalyst	100%	85%
Lifetime of catalyst, years	<5	10

ondary reforming stage through the outer shells of the reactor (Fig. 3). As applied to the process for the production of H_2 (including for NH_3), this allows a significant (20–30%) increase in its productivity [174, 175] and energy efficiency (a reduction of fuel consumption by up to 0.66 Gcal per 1 t of ammonia [175] or by ≈14% [8]), and minimization of excess steam production compared with conventional schemes (Table 5). Redistribution of the load between the primary and heat exchange reformers also leads to a noticeable decrease in NO_x and CO_x emissions [174, 175].

In some cases, for low-capacity NH_3 production processes (250–500 tpd), it is even possible to remove the conventional tubular steam reformer, e.g., in KBR's KAAPlus™ or PURIFIERplus™ processes using the KRES™ heat exchange reformer [8], or in Thyssen Krupp's A-04 series process with GHR heat exchange reactors (Johnsson Matthey) [176]. In this case, the heat exchange reformer and the ATR reactor operate in parallel: air and 60–70% of the mixture of SG and steam are fed to the ATR reactor, and the remaining 30–40% are fed to the heat exchange reformer. The heat for the reaction in it is provided by SG supplied from the ATR reactor. A 44% reduction in the capacity of the ATR reactor burner, which is possible during the KBR's process in this case, allows a 56% reduction in NO_x and CO_x emissions [8].

The capital costs, in turn, increase disproportionately when the process productivity for ammonia increases above 4000 tpd due to the addition of an autothermal or heat exchange reformer into the scheme. To solve this problem, the tubular steam reforming reactor is replaced by an ATR reactor using oxygen instead of air. In this case, for example, in the SynCOR Ammonia™ process announced in 2017 by Haldor Topsoe, the productivity of one unit can reach 6000 tpd or more [94]. In this process, steam consumption is reduced by 80% due to the low steam : carbon ratio (0.6 instead of 3 for steam reforming). The use of liquid nitrogen washing technology for SG purification instead of methanation reduces the capital costs by ~14%.

In recent years, the majority of licensors (KBR, Haldor Topsoe, Lurgi, Uhde, Johnson Mat-

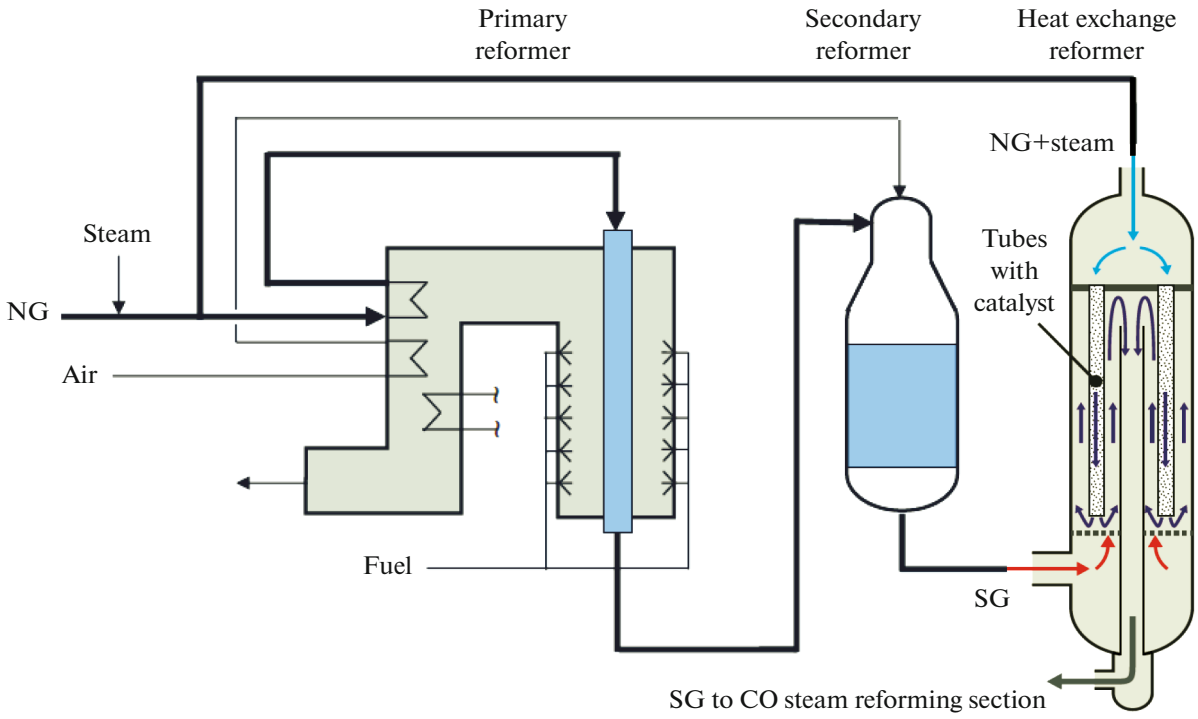

Fig. 3. One of the simplified flow diagrams for SG production using a heat exchange reformer (adapted from [123].

Table 5. Characteristics of various configurations of H_2 production sections at Haldor Topsoe plants for ammonia production with an output of 1600 tpd

Characteristic	Conventional scheme	Scheme with a heat exchange reformer (HTER)
Fuel consumption, m^3/h	15000	10500
Excess steam, t/h	60	0
Reduced fuel consumption, Gcal per 1 t of NH_3	–	0.61

they/DPT) have offered processes for the production of methanol and ammonia at the same plants. This allows quick response to the changing demand and composition of feedstock for SG production. In China, technologies with alternating production of one of the target products in separate parallel lines are widely used. In this case, however, there is always unused facility with its own warehouses and logistics support. Therefore, more widespread processes are those in which the feedstock for the production of H_2 in the ammonia synthesis is the purge gas from methanol production, which in conventional processes is directed for combustion in a reforming furnace [8, 12, 177]. Thus, in the Integrated Methanol Ammonia Production (IMAP™) process offered by Haldor Topsoe, a simplified diagram of which is shown in Fig. 4, with a total productivity of up to 3200 tpd, the ratio between the produced amounts of methanol and ammonia can be varied in very wide ranges, which allows saving from 10 to 25% of capital investments and up to 4% of operating costs [12]. A similar KBR's process (JM-KBR Ammonia Methanol) is based on the separate production of methanol (JM SMR from Johnson Matthey) and ammonia (KBR's Purifier™) [178]. According to one of these technologies, which allow a reduction in NG consumption per 1 ton of produced NH_3 below the value determined by the reaction stoichiometry at a 100% yield at all stages (631 and 660 $n.m^3$, respectively [13]), at present Metafrax (Gubakha) is building a complex for the production of ammonia, urea, and melamine.

Thus, the variety of processes existing on the market of processes for the production of ammonia, whose configurations are largely determined by the availability and price of feedstock and energy resources, makes it possible to choose the optimum options for SG production for the majority of regions.

2.6. Main Peculiarities of the Development of Industrial SG Production Technologies for Methanol

The overwhelming majority of industrial processes for the production of methanol are based on the catalytic reaction between CO and H_2, forming syngas: $CO + 2H_2 = CH_3OH$.

Syngas, in turn, is produced by one of the NG reforming or coal gasification processes.

Growth in methanol production in recent years is mainly provided by plants with a capacity of 1 to 5 million t/year (so-called megamethanol plants). For example, in the United States, an increase in methanol production from 1675 thousand tons in 2013 to 12370 thousand tons in 2018 resulted from the launch of seven plants with a total capacity of 9790 thousand tons per year, six of which used NG as feedstock. Of the 16194 thousand tons of methanol produced in 2018 in the Middle East, 11670 thousand tons were obtained at megamethanol plants. This tendency is due to a noticeable decrease in the prime cost of methanol compared to that at small plants, reaching less than $100/t in regions with a low cost of NG (Middle East, Russia) [19]. In addition to the low cost of NG, this reduction in the prime cost is determined by a significant decrease in capital investments per unit capacity. Selection and optimization of process conditions for methanol production are very important

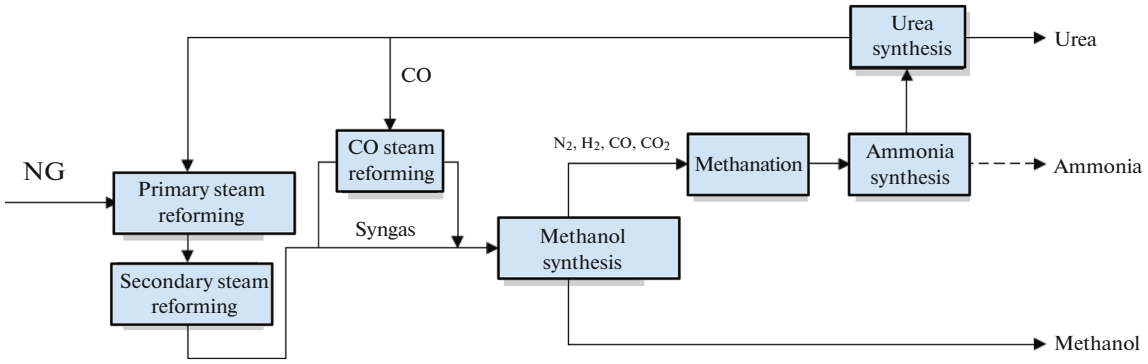

Fig. 4. Schematic flow diagram for combined production of methanol and ammonia (Haldor Topsoe) [12].

Table 6. Parameters of various processes in SG production with a methanol capacity of 5000 t/day (adapted from [29])

	Toyo	Lurgi	Haldor Topsoe	Johnson Matthey/Davy
SG capacity, thousand m^3/day	1415	1132	1132	1132
First reactor (steam reforming)				
H_2O : C	3.2	2.8	1.5	1.5
H_2 : CO in SG	2.97	No data	No data	No data
CH_4 at the outlet, %	3.2	12.5	36.5	36
Second reactor	–	ATR*	ATR**	ATR
CH_4 at the outlet, %	3.2	2.2	1.0	1.5
SN	2.97	2.03	2.02	2.02
H_2 : CO in SG	3.2	No data	2.91	3.0

* Parallel arrangement of the steam and autothermal reforming reactors with approximately halved gas flows.
** Sequential arrangement of the steam and autothermal reforming reactors.

because of the high contribution of the SG production stage to the cost of methanol production. The construction and maintenance costs of tubular reformers with a capacity exceeding 3000 tpd of methanol increase disproportionately, which does not allow saving due to scaleup. This is primarily determined by the technological problem in the functioning of devices with a large number of tubes. As in the case of SG production for ammonia, the problem in increasing the productivity is solved by introducing a secondary reforming stage using ATR reactors. Due to the higher temperature in the ATR reactor, the methane slip is reduced to almost zero (Table 6), and the heat released during the reaction can be used to perform the steam reforming reaction [29]. In addition, the CO selectivity significantly increases. Due to this, H_2 : CO and the stoichiometric number (SN = ($[H_2]$–$[CO_2]$)/($[CO]$+$[CO_2]$) in SG approach the optimum values for methanol synthesis equal to 2 and 2.0–2.08, respectively, while in steam reforming of NG, H_2 : CO ≥ 3 (Table 1) and SN = 2.8–3.0 [29, 179]. In one-stage processes, it is required that some part of H_2 is separated from SG, which is further used as a fuel, or CO_2 should be added to SG. The latter requirement is advantageous only if there is an ammonia production nearby where CO_2 is separated from SG to leave pure H_2. A decrease in the degree of methane reforming in the tubular reformer in combined schemes can significantly reduce the steam : methane ratio at the reactor inlet (Table 6) to 0.6–0.8 typical of Haldor Topsoe's SynCOR™ process. This accordingly significantly reduces the cost of vapor compression.

On the other hand, an air separation unit is often required for the operation of an ATR reactor [179, 180].

The cost of SG obtained as a result of steam reforming of NG (developed by Toyo, Japan) or the combined process including the combination of steam and autothermal reforming of NG (the processes of Lurgi, Haldor Topsoe, and Johnson Matthey/Davy) in the schemes with parallel or sequential arrangement of steam reforming reactors and ATR (Table 6) was calculated in [29].

The calculations showed that the total capital investments required for the construction of the Toyo plant with an SG capacity sufficient to produce 5000 tpd of methanol (≈518 million USD in 2013 prices) is 8–9% higher than for the Lurgi and Haldor Topsoe plants and 23% higher than for the Johnson Matthey/Davy plant. Although the cost of SG according to Toyo technology (235 cents/cbft) is 5–8% lower compared to that calculated for combined technologies, the cost of separation of excess H_2 by one of the known methods (e.g., using pressure swing adsorption) completely annihilates the advantage of this technology.

Thus, the use of steam reforming processes for SG production is economically advantageous only at small and medium-sized plants with a methanol capacity of up to 3000 tpd. The combined schemes (steam reforming + ATR) are used at plants with a methanol capacity of 2500 to 7000 tpd. Autothermal reforming is most appropriate for SG production at plants with a capacity of over 7000 tpd regardless of the source of feedstock [181]. It is exactly due to lower investment costs, water content in crude methanol (lower costs for product purification), and markedly lower total consumption of NG for SG production (Table 7) that the ATR process has almost completely replaced the combined schemes at the largest-tonnage plants [180, 182].

When NG with a relatively high content of higher hydrocarbons is used as a feedstock for an ATR reactor, to provide the required H_2 : CO ratio, H_2 that remained unchanged in the methanol synthesis reactor is separated using PSA and recycled to the steam reforming reactor. However, at significant contents of heavier hydrocarbons in NG or when they are used as recycling feedstock, the amount of H_2 may be insufficient. In this case, exclusively combined reforming is

Table 7. Energy consumption and investment costs in various SG production technologies with a methanol capacity of 10000 tpd [179]

Characteristic	Two-stage (sequential) reforming	Parallel reforming	Autothermal reforming
NG consumption (feedstock), %	100	107	110
NG consumption (fuel), %	100	50	0
Steam for sale, %	100	156	69
Steam : carbon	1.8	2.5/0.6	0.6
O_2 consumption, %	100	104	142
CO : CO_2 in SG	2.7	4.7	6.3
H_2O in crude methanol, vol %	13	8	5
Investment costs, %	100	95	85

used, in which only some part of NG is fed to the steam reforming reactor, and then the resulting SG is mixed with the remaining NG and sent to the ATR reactor (used in Lurgi processes).

As is known, a Lurgi demonstration plant with a methanol capacity of 10000 tpd (GigaMethanol process) is being constructed in Freiburg (Germany). The scaleup problem in this project was solved by increasing the pressure of the SG production process (ATR) to 100 kgf/cm^2, which makes it possible to reduce the SG volume as there are limitations on the size of some special equipment such as taps, valves, etc.).

Thus, the main trend in methanol industry in recent years is associated with an increase in the share of plants with a methanol capacity of above 3.5–5 thousand tpd (megamethanol production). The majority of these plants use NG as a feedstock. In addition to the low cost of feedstock (determined primarily by proximity to the production site and the cost of NG), the low cost of produced methanol obtained at these plants (less than $ 100/t) is due to significantly lower capital investments and operating costs per unit capacity. For the stage of syngas production from NG, this is achieved by using autothermal reforming units. All major licensors of this process have such technologies in their portfolio.

2.7. Current State of Production of Natural Gas Reforming Catalysts in Russia

The production of full-cycle catalysts for syngas or H_2 production by steam or steam-oxygen reforming of NG is historically concentrated at NIAP-Katalizator (Novomoskovsk) and Angarsk Plant of Catalysts and Organic Synthesis (AZKiOS), currently part of the structure of Rosneft. The NIAP-03-01Sh catalyst, a new version of the NIAP-03-01 catalyst, which has been successfully used for many years in steam and steam-air reforming of NG (only 30 loads), is characterized by higher specific activity, as well as reduced gas-dynamic resistance (30%) and bulk density (10%). This makes it possible to reduce the reactor charge and the pressure drop in it, or to increase the load on the unit without increasing the pressure drop. The thermostable catalyst NIAP-04-02 has been proposed for installation in the frontal protective layer of the secondary reforming reactor. In the K-905 D1 catalyst for reforming NG with a high content of higher hydrocarbons, additional promotion with rare earth elements (La) is used, which suppresses soot formation and does not lower the activity unlike alkaline promoters. As the enterprise produces only catalysts for low-temperature CO reforming, special attention is paid to the development of modern catalysts for the protective layer, including NTK-10-2LF (protection against droplet moisture, absorption of sulfur compounds and chlorine) [183].

After successful testing of the AKN-M steam reforming catalyst produced at AZKiOS on the H_2 production unit at Syzran Refinery [184], which confirmed its compliance with the level of world standards, Rosneft started using these catalysts in 2018 at Kuibyshev and Ryazan refineries. As a result, by 2020 the share of steam reforming catalysts at Rosneft refineries reached 77%. It is also known that the imported analogs were replaced with Angarsk catalysts at the hydrogen units of Bashneft-Ufaneftekhim, Bashneft-Novoil, and Syzran refinery [185]. Catalysts for medium-temperature steam CO reforming based on iron, chromium, copper, and manganese oxides were patented in 2017 by AZKiOS [186]; however, there is no information on the industrial use of the new brands of these catalysts.

Thus, at AZKiOS (Rosneft) there is production of competitive catalysts for steam and steam-oxygen reforming of NG, which have successfully replaced the imported analogs at H_2 production units at refineries. The catalysts produced by NIAP-Katalizator are mainly used at ammonia- and methanol-producing plants, which most likely use outdated technologies. There is no production of sorbents for H_2 purification by pressure swing adsorption in Russia.

CONCLUSIONS

Syngas production is a key stage in all industrial technologies natural gas conversion into large-scale products (ammonia, methanol, hydrogen, hydrocarbons). Its contribution to the prime cost of the final product reaches 70%; therefore, studies that reduce the material and energy consumption of this process are very important. The development of industrial processes in this direction mainly concerns both the optimization of technological schemes and the improvement of catalysts and sorbents for each stage.

The use of additional heat-exchange and autothermal reforming reactors in the conventional schemes with tubular NG steam reforming reactors makes it possible to work at lower H_2O : feedstock ratios and to reduce the total energy consumption and heat load on the primary reformer, which increases the service life of both the catalyst and the tubular part of the reactor. The introduction of a preliminary reformer in the technological scheme of the reactor increases the process flexibility in terms of the feedstock composition.

The present review analyzed the catalysts/sorbents used (compositions and preparation methods that ensure the maximum activity and stability, as well as sorption characteristics) for all stages of the process. In modern reactors, layer-by-layer loading of catalysts of different compositions is used at all stages of the process, which ensures the maximum activity and stability throughout the whole run. In steam reforming reactors, supported nickel catalysts with supports based on Mg(Ca)–Al–O, which are more resistant to sintering and carbonization, are installed in the frontal layers, followed by more active Ni/α-Al_2O_3 systems. Ni(+K)/support packs with alkaline additive contents decreasing along the layer length are also used. The use of preliminarily reduced nickel catalysts in the frontal layers of pre-reforming reactors provides reduced start-up time of the apparatus. The use of supports with zirconium oxide additives and an active component based on Ni alloys with platinum group metals provides high thermal stability of the catalysts in the frontal layers of the ATR reactor. Haldor Topsoe offers three-layer catalyst loading in reactors for low-temperature steam reforming of carbon monoxide according to the "high water resistance and chlorine capacity–maximum activity–heat resistance" principle. As is known, in units working at low steam : carbon monoxide ratios, systems based on Zn–Al–O are used instead of highly toxic chromium-containing catalysts for steam reforming.

Based on the results of the analysis, it can be concluded that the improvement of catalytic systems for producing syngas is aimed primarily at developing catalysts that are stable at low steam : gas ratios at all stages of the process. The EU decisions on the development of hydrogen energy and reductions of the carbon traces pose a new challenge, namely, reduction of carbon dioxide emissions. This may require further radical changes in syngas production technologies.

FUNDING

This work was financially supported by the Ministry of Science and Higher Education of the Russian Federation under the government contract at the Institute of Catalysis, Siberian Branch, Russian Academy of Sciences (project no. AAAA-A21-121011390010-7).

REFERENCES

1. BP Official Website, BP Energy Outlook, 2020. https://www.bp.com/content/dam/bp/business-sites/en/global/corporate/pdfs/energy-economics/energy-outlook/bp-energy-outlook-2020.pdf. Cited January 17, 2022.
2. Nexant Official Website. Natural Gas as C_1 Chemicals Feedstock—2016 Update, 2016. https://www.nexanteca.com/reports/natural-gas-c1-chemicals-feedstock-2016-update. Cited January 17, 2022.
3. Enerdata Official Website. https://yearbook.enerdata.ru/natural-gas/world-natural-gas-production-statistics.html. Cited April 12, 2021.
4. Devaney, M.T., *Natural Gas. (229.2000). Chemical Economics Handbook,* IHS Chemical, 2013. http://cdn.ihs.com/www/pdf/IHS-Chemical-Economics-Handbook-brochure-feb-2013.pdf. Cited January 17, 2022.
5. OECD Official Website, The Future of Petrochemicals. Towards More Sustainable Plastics and Fertilizers, 2018. https://www.oecd.org/publications/the-future-of-petrochemicals-9789264307414-en.htm. Cited January 17, 2022.
6. Aminev, S. Kh., *Vestn. Khim. Prom-sti,* 2016. http://vestkhimprom.ru/posts/glubokaya-pererabotka-gaza-i-nefti-kak-klyuch-resheniya-problemy-importozameshcheniya-v-oblasti-khimii-i-neftekhimii. Cited November 17, 2020.
7. Choudhary, T.V. and Vasant, R.C., *Angew. Chem., Int. Ed. Engl.,* 2008, vol. 47, pp. 1828–1847.
8. Trabulsy, J., *Ammonia, Process Evaluation and Research Planning,* Nexant Thinking™, 2014, report PERP-2014-6.
9. Haggin, J., *Chem. Eng. News,* 1992, vol. 70, pp. 33–35.
10. *Vodorodnaya ekonomika: novye nadezhdy na uspekh* (Hydrogen Economics: New Hopes for Success), Moscow: Anal. Tsentr Pravit. Ross. Fed., 2019. https://ac.gov.ru/news/page/vodorodnaa-ekonomika-novye-nadezdy-na-uspeh-22857. Cited January 17, 2022.
11. Ramos, L. and Zeppieri, S., *Fuel,* 2013, vol. 110, pp. 141–152.
12. Haldor Topsoe Official Website. Ammonia/Co-production. https://www.topsoe.com/processes/ammonia/co-production. Cited November 1, 2020.
13. *Proizvodstvo ammiaka, mineral'nykh udobrenii i neorganicheskikh kislot. Informatsionno-tekhnicheskii spravochnik po nailuchshim dostupnym tekhnologiyam* (Production of Ammonia, Mineral Fertilizers, and Inorganic Acids. Information and Technical Handbook

on the Best Available Technologies), Moscow: Byuro NDT, 2019.

14. Zhigareva, G.V., *Vestn. Khim. Prom-sti,* 2019. http://vestkhimprom.ru/posts/ammiak-istoriya-sovremennost-i-perspektivy-razvitiya-v-rossii. Cited May 20, 2021.
15. RUPEC Official Website. http://www.rupec.ru/news/41274/. Cited September 11, 2020.
16. METARAX CHEMICALS Official Website. http://www.metafrax.ru/ru/p/128. Cited September 11, 2020.
17. SCHEKINOAZOT United Chemical Company Official Website. http://n-azot.ru/news.php?news_id=1510&lang=RU. Cited September 11, 2020.
18. Davis, S., *Petrochemical Industry Overview (350.000). Chemical Economics Handbook,* IHS Chemical, 2015.
19. Sriram, P., Nash, M., and Maronneaud, O., *Methanol (674.5000). Chemical Economics Handbook,* IHS Chemical, 2014.
20. Argusmedia Official Website. Global Methanol Demand, 2018. https://www.argusmedia.com/-/media/090F0C06A6A396546B3698F913E6A1AC54DEAE8E. Cited November 6, 2020.
21. REFINITIV Official Website. https://www.refinitiv.ru/blog/market-insights/kratkij-obzor-rossijskogo-rynka-metanola-po-itogam-2019/. Cited May 20, 2021.
22. SCHEKINOAZOT United Chemical Company Official Website. http://n-azot.ru/about.php. Cited November 9, 2020.
23. Da Silva, M.J., *Fuel Process. Technol.,* 2016, vol. 145, pp. 42–61.
24. Ott, J., Gronemann, V., Pontzen, F., Fiedler, E., Grossmann, G., Kersebohm, B., Weiss, G., and Witte, C., in *Ullmann's Encyclopedia of Technical Chemistry,* Weinheim: Wiley-VCH, 2013.
25. BCC Research Official Website. Merchant Hydrogen: Industrial Gas and Energy Markets, 2015, report CHM042C. https://www.bccresearch.com/market-research/chemicals/merchant-hydrogen-industrial-gas-market-chm042c.html. Cited January 17, 2022.
26. *GasWorld. Rossiya i SNG,* 2014, no. 34, pp. 20–23. https://www.google.com/url?q=https://gasworld.ru/uploads/issues/d/2014/27052014_120941.pdf&sa=U&ved=2ahUKEwjvzbbzo7n1AhVRAxAIHRMUBy8QFnoECAQQAg&usg=AOvVaw0r5a0yzlHdOpyD4Cgrt9kr
27. CREON Energy Official Website. http://www.creonenergy.ru/consulting/detailConf.php?ID=101824. Cited July 15, 2017.
28. Meleloe, K. and Walwyn, D., *S. Afr. J. Bus. Manage.,* 2016, vol. 47, no. 3, pp. 63–72.
29. Naqvi, S.N., *Synthesis Gas Production from Natural Gas Reforming,* IHS Chemical, 2013, report PEP148B.
30. You, Y.W., Lee, D.G., Kim, K.H., Oh, M., and Lee, C.H., *Chem. Eng. Sci.,* 2012, vol. 68, pp. 413–423.
31. Hydrocarbon Processing Constructions Boxscore Database. https://www.constructionboxscore.com/project-news/air-products-to-build-new-texas-methane-reformer-for-downstream-users.aspx. Cited November 23, 2020.
32. Air Liquide Official Website. https://www.airliquide.com/industry/chemicals. Cited November 3, 2020.
33. Linde Engineering Official Website. https://www.linde-engineering.com/en/process-plants/hydrogen_and_synthesis_gas_plants/gas_generation/steam_reforming/index.html. Cited November 23, 2020.
34. Trabulsy, J. and Chu, R., *Hydrogen Production in Refineries,* Nexant Thinking™, 2013, report PERP 2013S3.
35. McWilliams, A., *Catalysts for Environmental and Energy Applications,* BCC Research, 2015, report CHM020E.
36. Rostrup-Nielsen, J.R. and Rostrup-Nielsen, T., Large-scale Hydrogen Production. https://www.topsoe.com/sites/default/files/topsoe_large_scale_hydrogen_produc.pdf. Cited June 6, 2017.
37. US Patent 7449167, 2008.
38. Kumar, A., Baldea, M., and Edgar, T.F., *Comput. Chem. Eng.,* 2017, vol. 105, pp. 224–236.
39. Brunson, R., Flessner, U., and Morse, P., *Catalysis,* 2013, pp. 41–49. https://ru.scribd.com/document/398823433/2013-catalysis#. Cited January 17, 2022.
40. US Patent 5685890, 1997.
41. US Patent 5753143, 1998.
42. US Patent 6984371, 2006.
43. US 2009/02204113, 2009.
44. *Hydroprocessing of Heavy Oils and Residua,* Ancheyta, J., and Speight, J.G., Eds., Boca Raton, FL: CRC Press/Taylor & Francis Group, 2007.
45. US Patent 7767619, 2010.
46. US Patent 7771586, 2010.
47. Süd-Chemie India Official Website. http://www.sud-chemie-india.com/uploads/documents/ammonia/1.%20%20Reforming%20Catalyst.pdf. Cited August 2, 2017.
48. Haldor Topsoe Official Website. RC-67 Titan™. https://www.topsoe.com/products/catalysts/rc-67-titantm?hsLang=en. Cited May 26, 2021.
49. Yamazaki, O., Tomishige, K., and Fujimoto, K., Appl. Catal., A., 1996, vol. 136, pp. 49–56.
50. WO Patent 2014/048740, 2014.
51. US Patent 2015/0231608, 2015.
52. *Handbook of Petroleum Refining,* Speight, J.G., Ed., Boca Raton, FL: CRC Press/Taylor & Francis Group LLC, 2017.
53. Haldor Topsoe Official Website. Hydrogen. https://www.topsoe.com/ru/tehnologii/vodorod. Cited July 20, 2017.
54. Haldor Topsoe Official Website. Hydrogen/Reforming. https://www.topsoe.com/ru/processes/hydrogen/reforming. Cited May 20, 2021.
55. Meloni, E., Martino, M., and Palma, V., *Catalysts,* 2020, vol. 10, pp. 352–390.
56. Cross, J., Jones, G., and Kent, M.A., *Nitrogen + Syngas,* 2016, vol. 341, pp. 40–48.
57. Clariant International Official Website. Catalysts for Syngas 2010. http://www.clariant.com/Catalysts. Cited July 20, 2018.
58. US Patent 7622058, 2009.
59. WO Patent 2016/047504, 2016.

60. Pashchenko, D., *Energy Convers. Manage.,* 2019, vol. 185, pp. 465–472.
61. Clariant Official Website. Clariant ReforMax LDP Plus: a new generation of reforming catalysts with ultra-low pressure drop. https://www.clariant.com/ru-RU/Corporate/News/2017/03/Clariants-ReforMax-LDP-Plus-a-new-generation-of-reforming-catalysts-with-ultralow-pressure-drop. Cited January 17, 2022.
62. Librera, C., *PTQ,* Q2 2020, pp. 43-47. https://cdn.digitalrefining.com/data/page/fck/magazine/113.pdf. Cited January 17, 2022.
63. US Patent 4861745, 1989.
64. Ratnasamy, C. and Wagner, J.P., *Catal. Rev.,* 2009, vol. 51, pp. 325–440.
65. Aasberg-Petersen, K., Dybkjær, I., Ovesen, C.V., Schjødt, N.C., Sehested, J., and Thomsen, S.G., *J. Nat. Gas Sci. Eng.,* 2011, vol. 3, no. 2, pp. 423–0459.
66. Busca, G., in *Heterogeneous Catalytic Materials,* New York: Elsevier, 2014, pp. 345–374. https://doi.org/10.1016/B978-0-444-59524-9.00010-9
67. Li, Q., Ma, W., He, R., and Mu, Z., *Catal. Today,* 2005, vol. 106, pp. 52–56.
68. Natesakhawat, S., Wang, X., Zhang, L., and Ozkan U.S., *J. Mol. Catal. A Chem*., 2006, vol. 260, pp. 82–94.
69. EP Patent 1149799, 2001.
70. EP Patent 1445235, 2004.
71. Clariant Official Website. Clariant introduces Shift-Max® 120 HCF: New HTS catalyst with essentially no hexavalent chromium. https://www.clariant.com/ru-RU/Corporate/News/2014/09/Clariant-introduces-ShiftMax-reg–120-HCF–New-HTS-catalyst-with-essentially-no-hexavalent-chromium. Cited May 13, 2021.
72. Gines, M.J.L., Amadeo, N., Laborde, M., and Apesteguia, C.R., *Appl. Catal., A,* 1995, vol. 131, pp. 283–296.
73. US Patent 4835132, 1987.
74. WO Patent 2003/082468 A1, 2003.
75. US Patent 2010/0102278, 2010.
76. US Patent 2010/0112397, 2010.
77. US Patent 6693057, 2004.
78. US Patent 6627572, 2006.
79. US Patent 4863894, 1989.
80. US Patent 9492809, 2016.
81. US 2009/0149324, 2009.
82. Reddy, G.K. and Smirniotis, P.G., in *Water Gas Shift Reaction,* New York: Elsevier, 2015, pp. 1–20. https://doi.org/10.1016/B978-0-12-420154-5.00001-2
83. Tanaka, Y., Utaka, T., Kikuchi, R., Sasaki, K., and Eguchi, K., *Appl. Catal., A,* 2003, vol. 242, pp. 287–295.
84. EP Patent 2 599 541, 2011.
85. WO Patent 2013/079323, 2013.
86. Wang, X. and Gorte, R.J., *Appl. Catal., A,* 2003, vol. 247, pp. 157–162.
87. Panagiotopoulou, P. and Kondarides, D.I., *Catal. Today,* 2006, vol. 112, pp. 4952.
88. Gorte, R.J. and Zhao, S., *Catal. Today,* 2005, vol. 104, pp. 18–24.
89. Choung, S.Y., Ferrandon, M., and Krause, T., *Catal. Today,* 2005, vol. 99, pp. 257–262.
90. Radhakrishnan, R., Willigan, R.R., Dardas, Z., and Vanderspurt, T.H., *Appl. Catal., B,* 2006, vol. 66, pp. 23–28.
91. Pinaeva, L.G., Sadovskaya, E.M., Ivanova, Yu.A., Kuznetsova, T.G., Prosvirin, I.P., Sadykov, V.A., Schuurman, Y., van Veen, A.C., and Mirodatos, C., *Chem. Eng. J.,* 2014, vol. 257, pp. 281–291.
92. US Patent 8119099, 2012.
93. Haldor Topsoe Official Website. Hydrogen/CO Shift. https://www.topsoe.com/ru/processes/hydrogen/co-shift. Cited May 12, 2021.
94. Dahl, P.J., Speth, C., Jensen, A.E.K., Symreng, M., Hoffmann, M.K., Han, P.A., and Nielsen, S.E., New SynCOR Ammonia™ Process. https://info.topsoe.com/new-syncor-ammonia-process-wp-dlp. Cited April 29, 2021.
95. http://www.jmcatalysts.cn/en/pdf/HydrogenTech-BrochFeb2007.pdf. Cited December 23, 2018.
96. https://matthey.com/-/media/files/markets/jm-ammonia-market-brochure-c2018.pdf. Cited May 13, 2021.
97. Xiao, J., Mei, A., Tao, W., Ma, S., Bénard, P., and Chahine, R., *Energies,* 2021, vol. 14, pp. 2450–2464.
98. Grande, C.A., in *Hydrogen Science and Engineering: Materials, Processes, Systems and Technology,* Stolten, D. and Emonts, B., Eds. Weinheim: Wiley-VCH, 2016, pp. 491–508.
99. *Separation Technology R&D Needs for Hydrogen Production in the Chemical and Petrochemical Industries,* 2005. https://elearn.ing.unipi.it/pluginfile.php/157407/mod_resource/content/1/h2_report.pdf. Cited January 17, 2022.
100. Chou, C., Chen, F., Huang, Y.J., and Yang, H., *Chem. Eng. Trans.,* 2013, vol. 32, pp. 1855–1860.
101. Ebner, A.D. and Ritter, J.A., *Sep. Sci. Technol.,* 2009, vol. 44, pp. 1273–1421.
102. Hao, G.P., Li, W.C., and Lu, A.H., *J. Mater. Chem.,* 2011, vol. 21, pp. 6447–6451.
103. Di Biase, E. and Sarkisov, L., *Carbon,* 2015, vol. 94, pp. 27–40.
104. Azpiri Solares, R.A., dos Santos, D.S., Ingram, A., and Wood, J., *Fuel,* 2019, vol. 253, pp. 1130–1139.
105. Lopes, F.V.S., Grande, C.A., Ribeiro, A.M., Oliveira, E.L.G., Loureiro, J.M., and Rodrigues, A.E., *Ind. Eng. Chem. Res.,* 2009, vol. 48, no. 8, pp. 3978–3990.
106. Regufe, M.J., Tamajon, J., Ribeiro, A.M., Ferreira, A., Lee, U.H., Hwang, Y.K., Chang, J.S., Serre, C., Loureiro, J.M., and Rodrigues, A.E., *Energy Fuels,* 2015, vol. 29, no. 7, pp. 4654–4664.
107. Agueda, V.I., Delgado, J.A., Uguina, M.A., Brea, P., Spjelkavik, A.I., Blom, R., and Grande, C., *Chem. Eng. Sci.,* 2015, vol. 124, pp. 159–169.
108. Huang, A., Chen, Y., Wang, N., Hu, Z., Jiang, J., and Caro, J., *Chem. Commun.,* 2012, vol. 48, no. 89, pp. 10981–10983.
109. Zhao, L., Primabudi, E., and Stolten, D., *Energy Procedia,* 2014, vol. 63, pp. 1756–1772.
110. Krishna, R. and Long, J.R., *J. Phys. Chem. C,* 2011, vol. 115, no. 26, pp. 12941–12950.

111. Masala, A., Vitillo, J.G., Mondino, G., Grande, C.A., Blom, R., Manzolic, M., Marshall, M., and Bordiga, S., *ACS Appl. Mater. Interfaces,* 2017, vol. 9, no. 1, pp. 455–463.

112. Britt, D., Furukawa, H., Wang, B., Glover, T.G., and Yaghi, O.M., *Proc. Natl. Acad. Sci. U.S.A.,* 2009, vol. 106, no. 49, pp. 20637–20640.

113. Xiang, S., He, Y., Zhang, Z., Wu, H., Zhou, W., Krishna, R., and Chen, B., *Nat. Commun.,* 2012, vol. 3, p. 954.

114. Grande, C.A., Águeda, V.I., Spjelkavik, A., and Blom, R., *Chem. Eng. Sci.,* 2015, vol. 124, pp. 154–158.

115. Grande, C.A., Blom, R., Andreassen, K.A., and Stensrød, R.E., *Energy Procedia,* 2017, vol. 114, pp. 2265–2270.

116. Al-Naddaf, Q., Thakkar, H., and Rezaei, F., *ACS Appl. Mater. Interfaces,* 2018, vol. 10, no. 35, pp. 29656–29666.

117. US Patent 8815208, 2014.

118. US Patent 9604200, 2017.

119. Ammonia Plant Performance. https://matthey.com/-/media/files/markets/jm-ammonia-market-brochure-c2018.pdf. Cited May 6, 2021.

120. Haldor Topsoe Official Website. RKA-10: Oxygen-Fired Secondary and Autothermal Reforming Catalyst. https://www.topsoe.com/products/catalysts/rka-10?hsLang=en. Cited May 21, 2021.

121. Hou, Z., Chen, P., Fang, H., Zheng, X., and Yashima, T., *Int. J. Hydrogen Energy,* 2006, vol. 31, pp. 555–561.

122. Yentekakis, I.V., Panagiotopoulou, P., and Artemakis, G., *Appl. Catal., B,* 2021, vol. 296. https://doi.org/10.1016/j.apcatb.2021.120210

123. Liu, W., Li, L., Lin, S., Luo, Y., Bao, Z., Mao, Y., Li, K., Wu, D., and Peng, H., *J. Energy Chem.,* 2022, vol. 65, pp. 34–47.

124. Liu, C., Ye, J., Jiang, J., and Pan, Y., *ChemCatChem,* 2011, vol. 3, pp. 529–541.

125. Nair, M.M. and Kaliaguine, S., *New J. Chem.,* 2016, vol. 40, pp. 4049–4060.

126. Xu, L., Miao, Z., Song, H., Chen, W., and Chou, L., *Catal. Sci. Technol.,* 2014, vol. 4, pp. 1759–1770.

127. Li, S. and Gong, J., *Chem. Soc. Rev.,* 2014, vol. 43, pp. 7245–7256.

128. Batiot-Dupeyrat, C., Gallego, G.A.S., Mondragon, F., Barrault, J., and Tatibouët, J.-M., *Catal. Today,* 2005, vol. 107, pp. 474–480.

129. De Sousa, F.F., de Sousa, H.S., Oliveira, A.C., Junior, M.C., Ayala, A.P., Barros, E.B., Viana, B.C., Josue Filho, M., and Oliveira, A.C., *Int. J. Hydrogen Energy,* 2012, vol. 37, pp. 3201–3212.

130. Le Saché, E., Pastor-Pérez, L., Watson, D., Sepúlveda-Escribano, A., and Reina, T., *Appl. Catal., B,* vol. 236, pp. 458–465.

131. Zubenko, D., Singh, S., and Rosen, B.A., *Appl. Catal., B,* 2017, vol. 209, pp. 711–719.

132. Bhattar, S., Abedin, Md. A., Kanitkar, S., and Spivey, J.J., *Catal. Today,* 2021, vol. 365, pp. 2–23.

133. Gao, Y., Chen, D., Saccoccio, M., Lu, Z., and Ciucci, F., *Nano Energy,* 2016, vol. 27, pp. 499–508.

134. Neagu, D., Oh, T.-S., Miller, D.N., Ménard, H., Bukhari, S.M., Gamble, S.R., Gorte, R.J., Vohs, J.M., and Irvine, J.T.S., *Nat. Commun.,* 2015, vol. 6, p. 8120.

135. Sun, Y., Li, J., Zeng, Y., Amirkhiz, B.S., Wang, M., Behnamian, Y., and Luo, J., *J. Mater. Chem. A,* 2015, vol. 3, pp. 11048–11056.

136. Tsekouras, G., Neagu, D., and Irvine, J.T.S., *Energy Environ. Sci.,* 2013, vol. 6, pp. 256–266.

137. Arbag, H., Yasyerli, S., Yasyerli, N., and Dogu, G., *Int. J. Hydrogen Energy,* 2010, vol. 35, pp. 2296–2304.

138. Damyanova, S., Pawelec, B., Arishtirova, K., Fierro, J., Sener, C., and Dogu, T., *Appl. Catal., B,* 2009, vol. 92, pp. 250–261.

139. Guo, J., Lou, H., Zhao, H., Chai, D., and Zheng, X., Appl. Catal., A, 2004, vol. 273, pp. 75–82.

140. Guo, J., Lou, H., and Zheng. X., *Carbon,* 2007, vol. 45, pp. 1314–1321.

141. Koo, K.Y., Roh, H.S., Seo, Y.T., Seo, D.J., Yoon, W.L., and Park, S.B., Appl Catal., A, 2008, vol. 340, pp. 183–190.

142. Cho, E., Lee, Y.H., Kim, H., Jang, E.J., Kwak, J.H., Lee, K., Ko, C.H., and Yoon, W.L., *Appl. Catal., A,* 2020, vol. 602. https://doi.org/10.1016/j.apcata.2020.117694

143. Fernandez, C., Miranda, N., García, X., Eloy, P., Ruiz, P., Gordon, A., and Jimenez, R., *Appl. Catal., B,* 2014, vol. 156, pp. 202–212.

144. Alirezaei, I., Hafizi, A., and Rahimpour, M., *J. CO2 Util.,* 2018, vol. 23, pp. 105–116.

145. Nagaoka, K., Seshan, K., Aika, K.-I., and Lercher, J.A., *J. Catal.,* 2001, vol. 197, pp. 34–42.

146. Dębek, R., Galvez, M.E., Launay, F., Motak, M., Grzybek, T., and Da Costa, P., *Int. J. Hydrogen Energy,* 2016, vol. 41, pp. 11616–11623.

147. Ozkara-Aydınoglu, S. and Aksoylu, A.E., *Catal. Commun.,* 2010, vol. 11, pp. 1165–1170.

148. Laosiripojana, N., Chadwick, D., and Assabumrungrat, S., *Chem. Eng. J.,* 2008, vol. 138, pp. 264–273.

149. Xu, B.Q., Wei, J.M., Yu, Y.T., Li, Y., Li, J.L., and Zhu, Q.M., *J. Phys. Chem. B,* 2003, vol. 107, pp. 5203–5207.

150. Morales Anzures, F., Salinas Hernández, P., Mondragón Galicia, G., Gutiérrez Martínez, A., Tzompantzi Morales, F., Romero Romo, M.A., and Pérez Hernández, R. *Int. J Hydrogen Energy,* 2021, vol. 46, no. 51, pp. 26224–26233. https://doi.org/10.1016/j.ijhydene.2021.05.073

151. Lou, Y., Steib, M., Zhang, Q., Tiefenbacher, K., Horvath, A., Jentys, A., Liu, Y., and Lercher, J.A., *J. Catal.,* 2017, vol. 356, pp. 147–156.

152. Swirk, K., Rønning, M., Motak, M., Grzybek, T., and Da Costa, P., *Int. J. Hydrogen Energy,* 2021, vol. 46, pp. 12128–12144.

153. Pompeo, F., Nichio, N.N., Ferretti, O.A., and Resasco, D., *Int. J. Hydrogen Energy,* 2005, vol. 30, pp. 1399–1405.

154. Wang, Y., Zhao, Q., Li, L., Hu, C., and Da Costa, P., *Appl. Catal., A,* 2021, vol. 617. https://doi.org/10.1016/j.apcata.2021.118120

155. Wang, N., Chu, W., Zhang, T., and Zhao, X.S., *Chem. Eng. J.,* 2011, vol. 170, pp. 457–463.

156. Lu, Y., Zhu, J., Peng, X., Tong, D., and Hu, C., *Int. J. Hydrogen Energy,* 2013, vol. 38, pp. 7268–7279.

157. Seok, S.H., Choi, S.H., Park, E.D., Han, S.H., and Lee, J.S., *J. Catal.,* 2002, vol. 209, pp. 6–15.

158. Luna, A.E.C. and Iriarte, M.E., Appl. Catal., A, 2008, vol. 343, pp. 10–15.

159. Liu, H., Hadjltaief, H.B., Benzina, M., Galvez, M.E., and Da Costa, P., *Int. J. Hydrogen Energy,* 2019, vol. 44, pp. 246–255.

160. Wang, J.B., Tai, Y.L., Dow, W.P., and Huang, T.J., *Appl. Catal., A,* 2001, vol. 218, pp. 69–79.

161. Yan, X., Hu, T., Liu, P., Li, S., Zhao, B., Zhang, Q., Jiao, W., Chen, S., Wang, P., Lu, J., Fan, L., Deng, X., and Pan, Y.X., *Appl. Catal., B,* 2019, vol. 246, pp. 221–231.

162. Alvarez-Galvan, M.C., Navarro, R.M., Rosa, F., Briceno, Y., Gordillo Alvarez, F., and Fierro, J.L.G., *Int. J. Hydrogen Energy,* 2008, vol. 33, pp. 652–663.

163. Gonzalez-Delacruz, V.M., Ternero, F., Pereñíguez, R., Caballero, A., and Holgado, J.P., *Appl. Catal., A,* 2010, vol. 384, pp. 1–9.

164. Liu, Z., Grinter, D.C., Lustemberg, P.G., Nguyen-Phan, T.D., Zhou, Y., Luo, S., Waluyo, I., Crumlin, E.J., Stacchiola, D.J., Zhou, J., Carrasco, J., Busnengo, H.F., Ganduglia-Pirovano, M.V., Senanayake, S.D., and Rodriguez, J.A., *Angew. Chem., Int. Ed.,* 2016, vol. 55, pp. 7455–7459.

165. Yu, M., Zhu, Y.A., Lu, Y., Tong, G., Zhu, K., and Zhou, X., *Appl. Catal., B,* 2015, vol. 165, pp. 43–56.

166. Charisiou, N., Siakavelas, G., Tzounis, L., Sebastian, V., Monzon, A., Baker, M., Hinder, S., Polychronopoulou, K., Yentekakis, I., and Goula, M., *Int. J. Hydrogen Energy,* 2018, vol. 43, pp. 18955–18976.

167. Kambolis, A., Matralis, H., Trovarelli, A., and Papadopoulou, C., *Appl. Catal., A,* 2010, vol. 377, pp. 16–26.

168. Ocsachoque, M., Pompeo, F., and Gonzalez, G., *Catal. Today,* 2011, vol. 172, pp. 226–231.

169. Guo, D., Lu, Y., Ruan, Y., Zhao, Y., Zhao, Y., Wang, S., and Ma, X., *Appl. Catal., B,* 2020, vol. 277, // *Appl. Catal. B Environ*. 2020. V. 277. https://doi.org/10.1016/j.apcatb.2020.119278

170. Horváth, A., Németh, M., Beck, A., Maróti, B., Sáfrán, G., Pantaleo, G., Liotta, L.F., Venezia, A.M., and La Parola, V., *Appl. Catal., A,* 2021, vol. 621. https://doi.org/10.1016/j.apcata.2021.118174

171. Han, K., Yu, W., Xu, L., Deng, Z., Yu, H., and Wang, F., *Fuel,* 2021, vol. 291. https://doi.org/10.1016/j.fuel.2021.120182

172. Marinho, A.L.A., Toniolo, F.S., Noronha, F.B., Epron, F., Duprez, D., and Bion, N., *Appl. Catal., B,* 2021, vol. 281. https://doi.org/10.1016/j.apcatb.2020.119459

173. Teh, L.P., Setiabudi, H.D., Timmiati, S.N., Aziz, M.A.A., Annuar, N.H.R., and Ruslan, N.N., *Chem. Eng. Sci.,* 2021, vol. 242. https://doi.org/10.1016/j.ces.2021.116606

174. TechnipFMC Parallel Reformer (TPR®). https://www.technipfmc.com/media/2qkb4se5/tpr-parallel-reformer_210x270_final_web.pdf. Cited April 28, 2021.

175. Sandberg, P., Optimal Performance—Integration of Haldor Topsoe Heat Exchange Reformer in Ammonia Plants. https://info.topsoe.com/hter-whitepaper, Cited November 10, 2020.

176. Thyssenkrupp Official Website. https://www.thyssenkrupp-industrial-solutions.com/. Cited November 10, 2020.

177. Thyssenkrupp Official Website. Ammonia Technology. https://ucpcdn.thyssenkrupp.com/_legacy UCPthyssenkruppBAIS/assets.files/products___services/fertilizer_plants/ammonium_sulphate_plants/brochure-ammonia_scr.pdf. Cited November 3, 2020.

178. KBR Official Website. https://www.kbr.com/en/solutions/technologies/process-technologies/ammonia-fertilizers-technologies. Cited November 1, 2020.

179. *Methanol: The Basic Chemical and Energy Feedstock of the Future,* Bertau, M., Offermanns, H., Plass, L., Schmidt, F., and Wernicke, H.-J., Eds., Berlin, Heidelberg: Springer, 2014.

180. Dahl, P.J., Christensen, T.S., Winter-Madsen, S., and King, S.M., *Proc. Nitrogen + Syngas Int. Conf. Exhib.,* 2014, pp. pp. 1–12.

181. Methanol and Derivatives. Proven technologies for Optimal Production. 2016. https://www.engineering-airliquide.com/sites/activity_eandc/files/2016/07/13/methanol_and_derivatives_brochure-june_2016.pdf. Cited November 21, 2020.

182. Aasberg-Petersen, K., Hansen, J.H.B., Christensen, T.S., Dybkjaer, I., Christensen, P.S., Nielsen, C.S., Madsen, S.E.L.W., and Rostrup-Nielsen, J.R., *Appl. Catal., A,* 2001, vol. 221, pp. 379–387.

183. Golosman, E.Z., Dul'nev, A.V., Efremov, V.N., Kruglova, M.A., Lunin, V.V., Obysov, M.A., Polivanov, B.I., Tkachenko, I.S., and Tkachenko, S.N., Katal. Prom-sti, 2017, no. 6, pp. 487–509.

184. Ovsienko, O.L., Nikul'shin, P.A., Karavanov, A.N., and Yushkin, V.A., Katal. Prom-sti, 2019, no. 2, pp. 142–148.

185. Rosneft Official Website. https://www.rosneft.ru/press/news/item/197399/. Cited June 23, 2021.

186. RF Patent 2677650, 2017.

Translated by L. Smolina